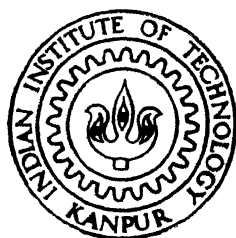# PERFORMANCE DEGRADATION OF WDM FIBER OPTIC SYSTEMS DUE TO FIBER NONLINEARITY EFFECTS, OPTICAL AMPLIFIER NOISE AND SWITCH CROSSTALK

by

MANINDER LAL SINGH

DEPARTMENT OF ELECTRICAL ENGINEERING

INDIAN INSTITUTE OF TECHNOLOGY KANPUR
JANUARY 1997

PERFORMANCE DEGRADATION OF WDM FIBER OPTIC SYSTEMS DUE TO FIBER NONLINEARITY EFFECTS, OPTICAL AMPLIFIER NOISE AND SWITCH CROSSTALK

*A Thesis submitted
in partial fulfilment of the Requirements
for the degree of*

MASTER OF TECHNOLOGY

By

MANINDER LAL SINGH

To the

DEPARTMENT OF ELECTRICAL ENGINEERING

## INDIAN INSTITUTE OF TECHNOLOGY KANPUR

January 1997

CERTIFICATE

This is to certify that the work contained in the thesis entitled 'PERFORMANCE DEGRADATION OF WDM FIBER OPTIC SYSTEMS DUE TO FIBER NONLINEARITY EFFECTS, OPTICAL AMPLIFIER NOISE AND SWITCH CROSSTALK' by **MANINDER LAL SINGH** has been carried out under my supervision and that this work has not been submitted elsewhere for a degree.

January, 1997

Dr. P. K. CHATTERJEE
Professor
Department of Electrical Engineering
Indian Institute of Technology
Kanpur
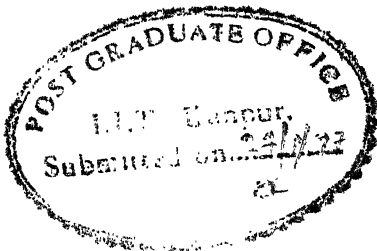
ABSTRACT

In this study, an attempt has been made to study the effects of the stimulated Raman Scattering (SRS), Four Wave Mixing (FWM), in-line optical amplifier spacing, Amplified Spontaneous Emission (ASE) noise accumulation, number of channels, channel separation, coupled power and optical space switch crosstalk on the performance of WDM fiber optic systems using dispersion shifted optical fibers in the 1.55 μm window. It is observed that for a WDM signal consisting of 4 channels with 4 nm channel separation, the maximum achievable system length for BER = 10^{-10} is 1200 km, 1950 km and 2600 km for the amplifier spacing of 100 km, 75 km and 50 km, respectively. On the other hand for the WDM signal consisting of 12 channels with 1 nm channel separation, for BER = 10^{-10}, the system length achieved is about 1700 km for both the 50 km and 75 km amplifier separations. So the choice of amplifier separation is dependent on both the number of channels and the channel separation in a WDM system. Also it is seen that increase in the coupled optical power does not always improve the system performance in terms of BER. Saturation in the BER value takes place for large coupled power. The effects of the switch crosstalk on the system performance is studied, and it has been noticed that for large number of space switches in an optical path, switches with crosstalk per cross point less than - 25 dB are preferable to keep the degradation of the system performance at acceptable limits.

ACKNOWLEDGEMENT

CONTENTS

. . .

LIST OF FIGURES

CHAPTER - 1

INTRODUCTION

With the emergence of broad band services like video conferencing, multimedia applications, video on demand etc., demand for networks with very high capacity is increasing. Networks incorporating conventional coaxial cables are finding it difficult to cope up with the day by day increasing demands on the network capacity enhancements. This has led to extensive research into high capacity optical networks. A single mode optical fiber used in optical network provides enormous bandwidth ($\approx$ 12.5 THz) in the 1.55 μm window. One way of exploiting this potential capacity of a single mode optical fiber is the use of Wavelength Division Multiplexing (WDM), in which signals of different wavelengths are multiplexed into a fiber such that the available bandwidth of the fiber is more efficiently used.

1.1 WAVELENGTH DIVISION MULTIPLEXING (WDM)

Fig. 1.1. gives a block schematic of a WDM system for a point to point link. The blocks labeled Tx are the optical sources generating optical signals at different wavelengths, i.e. λ_1, λ_2, ..., λ_N, depending upon the applied electrical signals. Combiner is a passive component, also called optical multiplexer, used to combine optical signals at different wavelengths into a single WDM signal, which consists of a number of copropagating optical signals at different wavelengths. This WDM signal is then coupled to an optical fiber for transmission. Erbium doped fiber amplifiers (EDFAs) are used at certain intervals along the fiber to amplify the WDM signal to compensate for the attenuation of the
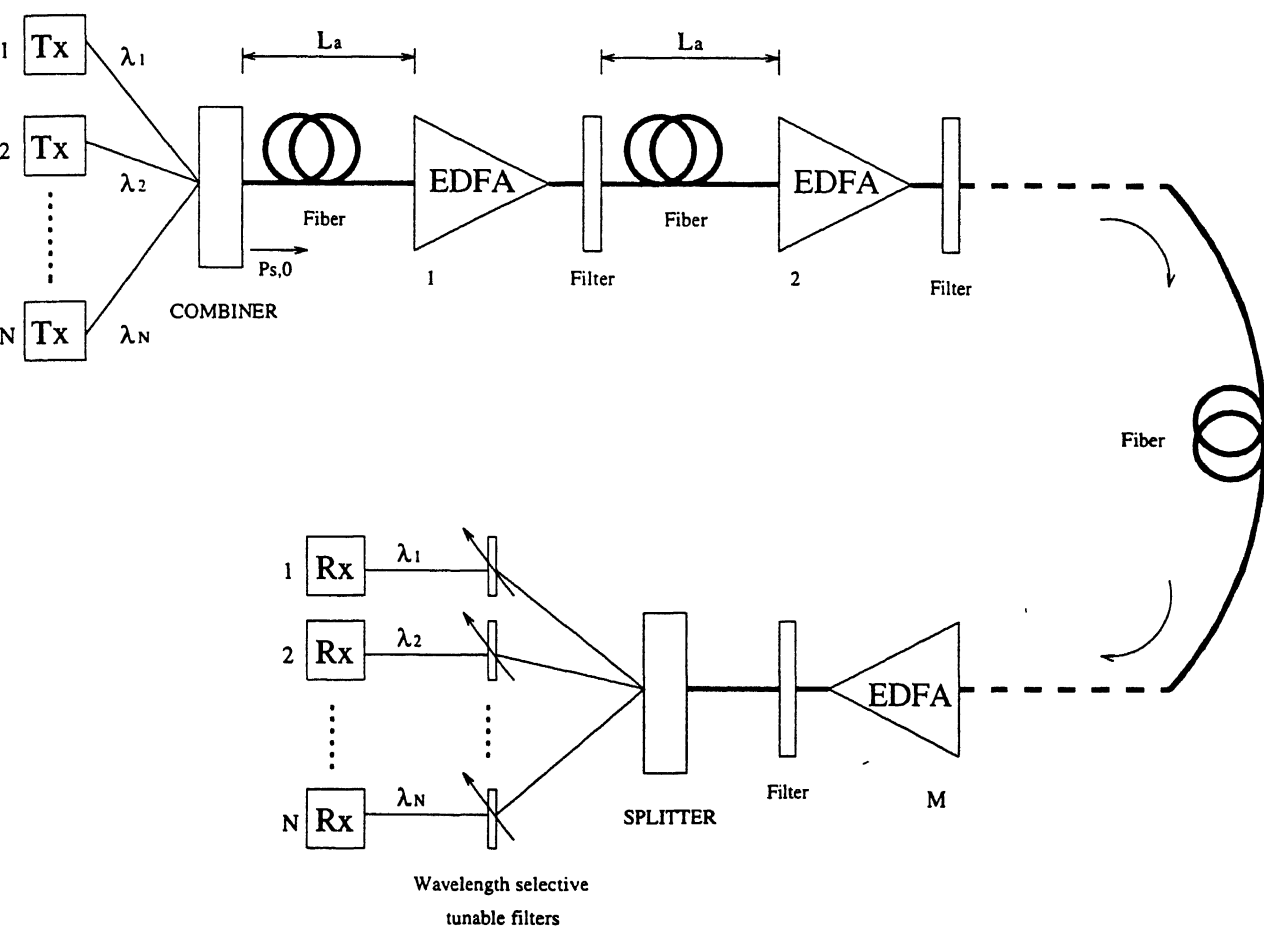
Fig. 1.1.   *N wavelength WDM fiber optic system with M inline optical amplifiers*

signal due to losses in fiber and connectors etc. EDFA amplifies
all the signals of different wavelengths in a WDM signal,
simultaneously, and removes the need for wavelength demultiplexing
and parallel regeneration at each repeater stage. This
significantly reduces the amount of equipment installed between
terminals. Filters at the output of each EDFA reject the
Amplified spontaneous Emission (ASE) noise outside the signal
band. Splitter is also a passive component. It makes use of 3dB
directional couplers for the power splitting. After this
wavelength selective tunable filters are used to separate out the
optical signals at the different wavelengths. Splitter and
wavelength selective tunable filters collectively form a
demultiplexer. Blocks labeled Rx are receivers used to convert
optical signals back to the electrical form. An additional
advantage of WDM is that it can be used to overcome the
transmission limitations due to dispersion associated with very
high capacity transmission in 1.55 μm window. In this case, for
example, the required capacity can be spread over a number of
channels simultaneously operating at different wavelengths.

1.2 ALL OPTICAL NETWORKS

Another major area of application of advanced optical
technology is that of switching and routing. At present all the
signal processing within the telecommunication networks is
realized electronically and optics remains limited to providing
the interconnection links between nodes. The broad band services
demand very high capacity networks, i.e. transmission of data at
the rate of several gigabits per second, but, at such rates it
becomes increasingly difficult to develop the necessary digital

lectronic circuits for switching.   In the recent years, herefore, there has been a rapidly growing interest in the study f all optical networks which provide both switching and ransmission within the optical domain.   The increasing interest n these networks is shown by the emphasis on optical networks ithin the RACE program in Europe and ARPA funded programs within he USA.   An European project COST 239 has been launched with the ain objective to evaluate the feasibility of an all optical etwork shown in Fig. 1.2, connecting major nodes across Europe 5].   The main features of this network are

- Network spans large geographical area with diameter in excess of 3000 km.

- Relatively small number of nodes (20)

- High capacity requirements in the longer term, for example, the number in brackets in Fig. 1.2 on the Amsterdam - Berlin indicates the 150 Gb/s point to point capacity.

- Each node represents a gateway into a national network and the aim is to design a transparent network that will carry all the international traffic between the nodes.

- Each node also incorporates an optical cross-connect switch, such that the overall interconnection of nodes can be reconfigured to support particular network requirements. Signals are routed through the network according to wavelength (wavelength routing). For example, in Fig. 1.2, wavelength λ_1 is used to establish a route between Dublin and Milan, while λ_2 is used to define a route between Doublin and Madrid. Schematic of the node architecture adopted by the RACE MWTN project is shown in Fig. 1.3.
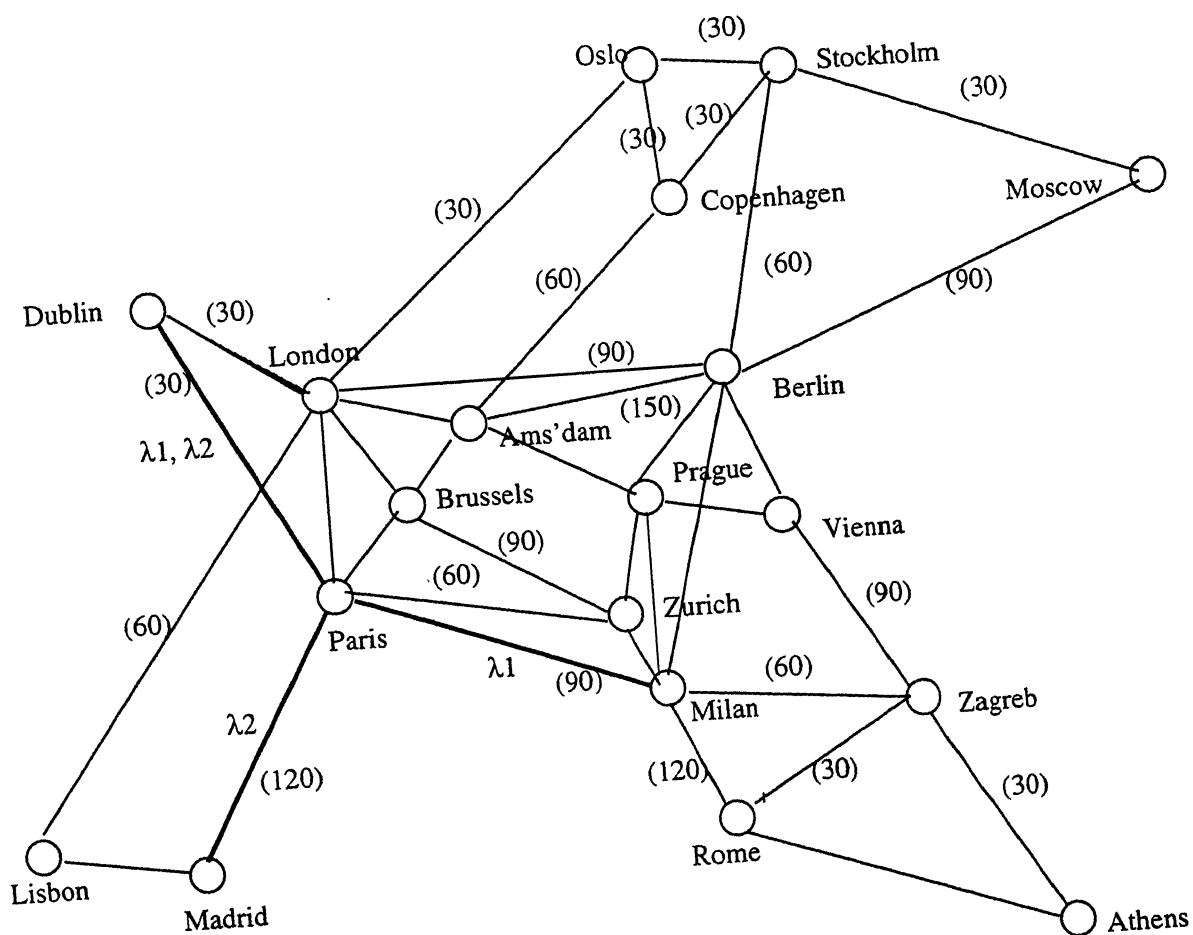
Fig. 1.2   A proposal for a European Optical Network
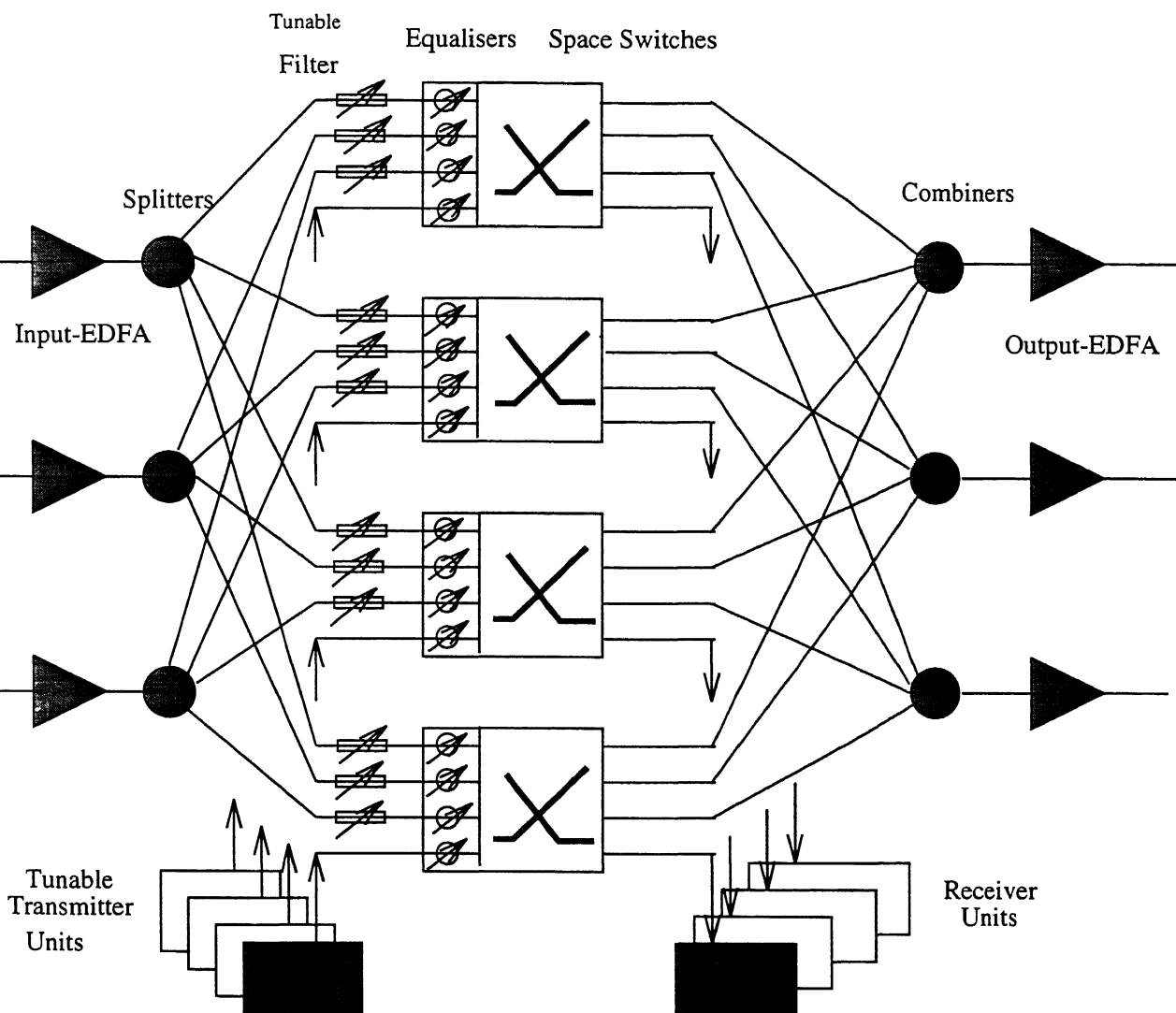
Fig. 1.3   *Schematic of the node architecture adopted by the RACE MWTN proje*

1.3 SOME PROBLEMS LIMITING THE PERFORMANCE OF WDM SYSTEMS

For WDM systems it may seem that as long as the signals are spectrally separate there is no cross talk. However, this may not always be the case. As a certain power per channel is required to ensure an adequate system error rate, the total power in the fiber (the sum of the individual powers) may be very high. Such high powers expose the fundamental nonlinear nature of optical fiber, which give rise to distortion and cross talk. Nonlinear effects [1] are function of the total power coupled to the fiber and the interaction length, they effectively constrain the maximum number of wavelengths possible over a particular distance. Some of the nonlinear effects which affect WDM systems are listed below:

- **Stimulated Raman Scattering (SRS) :** Light in the fiber interacts with molecular vibrations and scattered light is generated at a wavelength longer than that of the coupled light. In a WDM system energy is transferred from shorter to longer wavelengths.

- **Four Wave Mixing (FWM) :** This arises from the variation of fiber refractive index with optical power which causes an interaction between signals closely spaced in optical frequency, resulting in the generation of new signal components. This can be a serious impairment for systems using closely spaced wavelengths.

As mentioned earlier, SRS and FWM effects are particularly significant in WDM systems and their effect is to limit the product of number of wavelengths and transmission distance, i.e., the system capacity [5].

For optical networks with large distance, between any two

nodes, Say of the order of hundreds of kilometers, inline amplification is required. Erbium Doped Fiber Amplifiers (EDFAs) are used for this. As mentioned earlier that a single node optical fiber provides a bandwidth of ≃ 100 nm (≃ 12.5 THz) in 1.55 μm window, but, the use of EDFA as an inline amplifier reduces this bandwidth to ≃ 30 nm (≃3.7 THz).

Also cascading of many such amplifiers further reduces the end-to-end bandwidth of the system due to some deviation in the passband of EDFA. This problem can be reduced by the use of gain flattened amplifiers. Some techniques are given in [5] and [9]. The major problem in the use of EDFAs is that in a cascaded amplifier system, Amplified Spontaneous Emission (ASE) noise generated within each amplifier will accumulate along the chain and limit the number of amplifiers that may be cascaded. Optical filters at the output of the amplifiers are used to reject the ASE noise outside the signal band. Cascading of many filters further reduces the end-to-end system bandwidth. At the nodes, according to the requirements of a particular optical network, optical space switches are used for routing the signals to their destinations. These space switches introduce crosstalk among the signals, which degrades the system performance. Even the necessary equipment for WDM systems such as combiners and splitters may introduce crosstalk due to some manufacturing defects. So all the problems mentioned above make the designing of an efficient WDM system quite complicated and challenging [5].

1.4 PRESENT WORK

In future an optical network connecting the state capitals all over India may become a distinct possibility as the traffic is

pected to build up to such a values when these networks would

come a necessity. The present work is an effort made to study

e transmission limitations for a point-to-point link between two

des of such a futuristic network. A block schematic of such a

nk with the provision of space switching for wavelength routing

given in Fig. 1.4. Fig. 1.5 shows the wavelength routing at a

de with four input fibers each having signals with four

fferent wavelengths. Signals having wavelengths λ_1 to λ_4 in the

rst input fiber are processed in the receives at the local

rminal and the remaining twelve signals having wavelengths λ_5 to

6 arriving through the other three input fibers are routed to

ree outgoing fibers for further transmission through the

twork. Performance degradation of such a system due to the

fects of FWM, SRS, ASE noise accumulation, reduction of

d-to-end bandwidth due to cascaded filters and crosstalk in the

tical space switches is studied here. Considering all the above

entioned factors, the BER at the output of the receiver is

alculated for intensity modulation direct detection optical

ransmission.

5   THESIS LAYOUT

Chapter 2 deals with the undesirable effects of fiber

nlinearities such as FWM and SRS, and the limitations imposed by

ese effects on the system capacity.

In chapter 3 accumulation of Amplified spontaneous Emission

SE) noise in cascaded amplifier systems and a reduction in the

d-to-end system bandwidth due to cascaded filters is considered.

The limit on the maximum achievable system length, imposed by

e SRS and FWM effects has been discussed in Chapter 4.
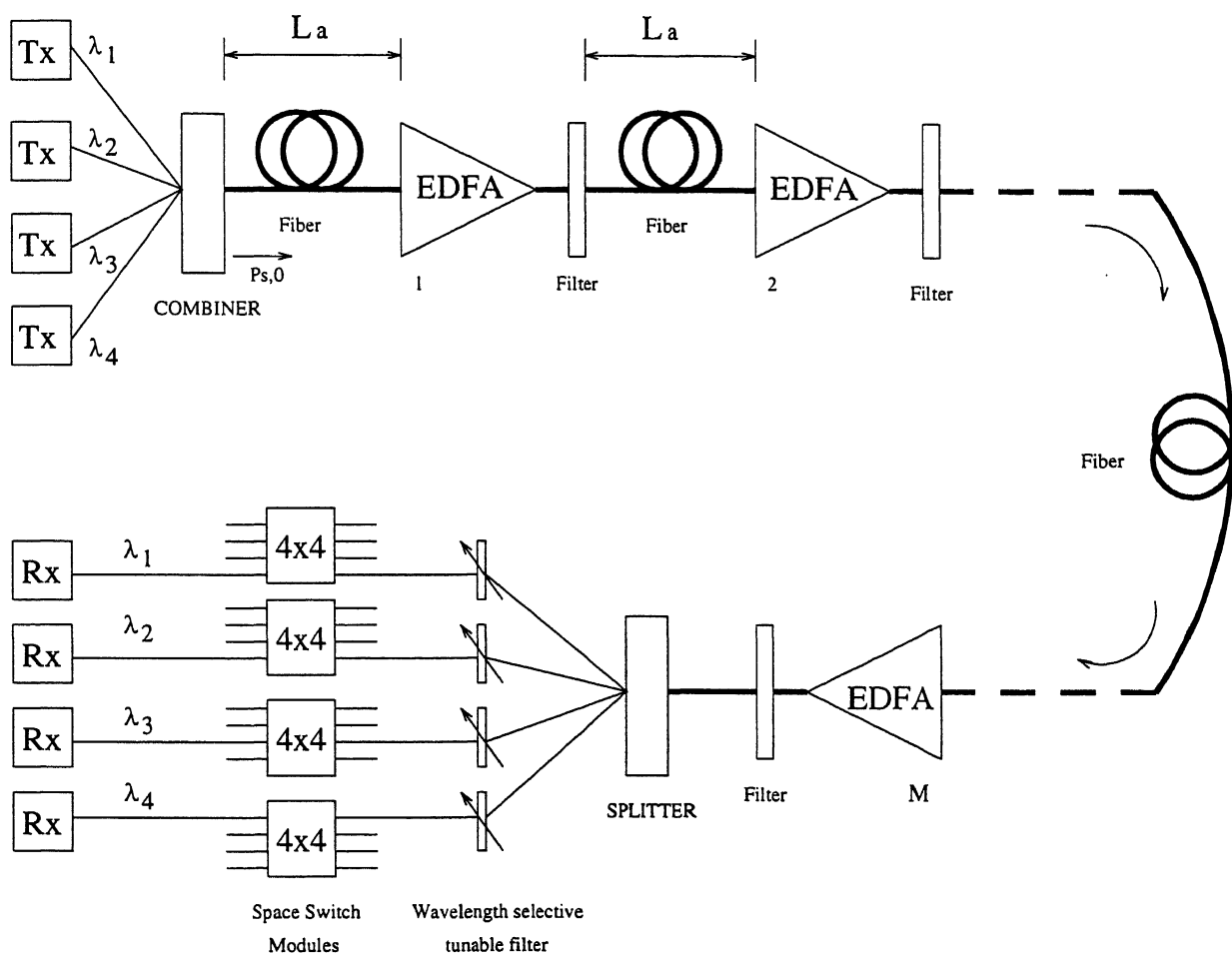
Fig.1.4   *4 wavelength WDM system with space switches*

FIBERS MUX
OUT

Space switches   DEMUX   FIBERS
                                    IN   1

Rx $\lambda 1$ 4x4 $\lambda 1 - \lambda 4$

                                                              2

Rx $\lambda 2$ 4x4 $\lambda 5 - \lambda 8$

                                                              3

Rx $\lambda 3$ 4x4 $\lambda 9 - \lambda 12$

                                                              4

Rx $\lambda 4$ 4x4 $\lambda 13 - \lambda 16$

MUX
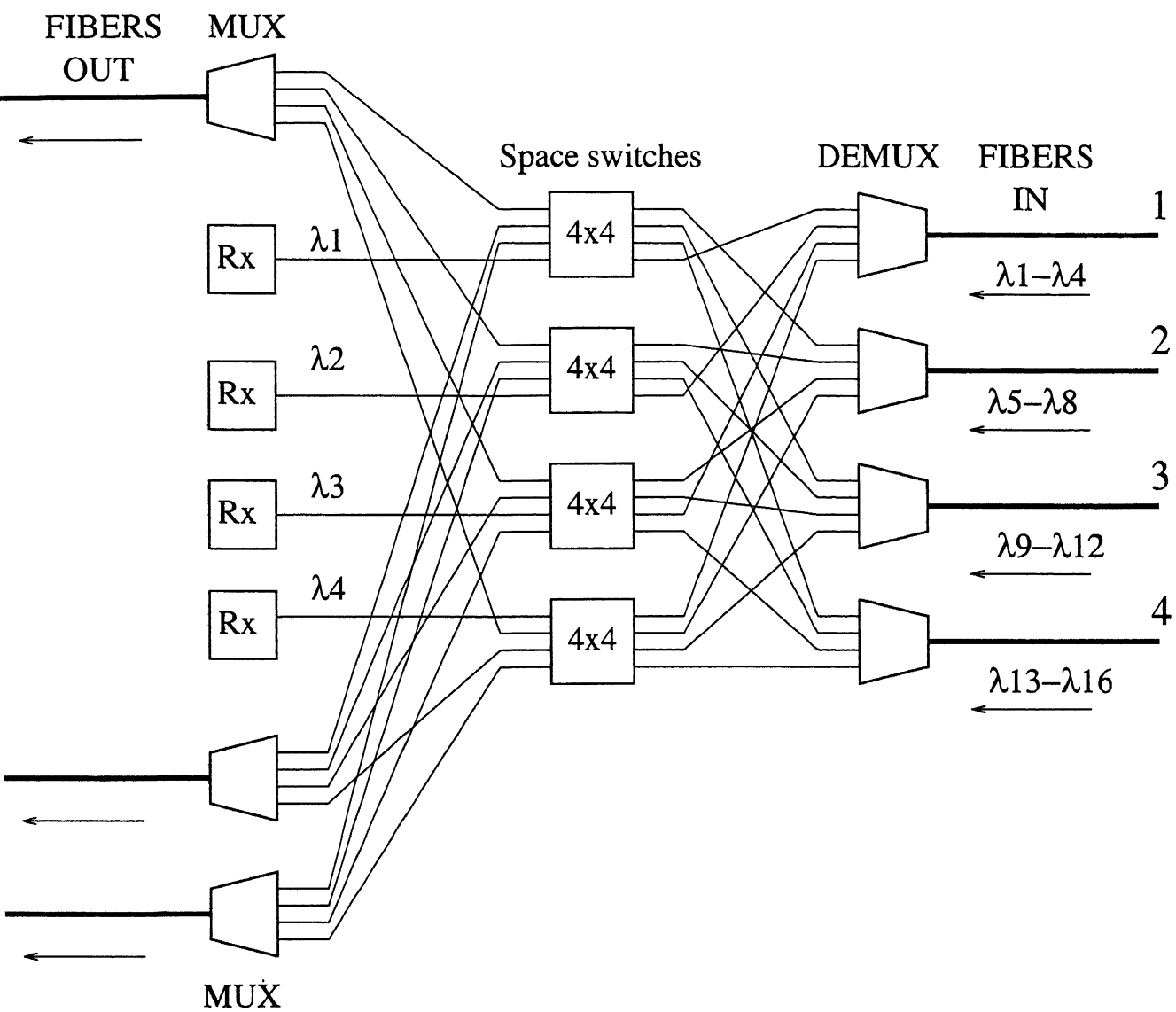
Fig. 1.5   Block schematic showing dynamic wavelength routing at a node

11

In Chapter 5 a theoretical analysis of WDM fiber optic system performance in terms of Bit Error Rate (BER) at the output of the receiver has been provided.

Degradation of the system performance due to crosstalk in the optical space switches is considered in Chapter 6.

Finally the study is concluded in Chapter 7.

CHAPTER - 2
SIGNIFICANT NONLINEARITIES IN WDM SYSTEM

Stimulated Raman Scattering (SRS) and Four Wave Mixing (FWM) are significant nonlinear effects in Wavelength Division Multiplexed (WDM) fiber optic systems. These effects limit the system capacity, i.e., the product of the number of channels and the transmission distance in such a system. FWM and SRS effects are discussed in this chapter and their effect on the number of channels and the system length have been shown.

2.1 STIMULATED RAMAN SCATTERING (SRS)

In SRS the coupled light in the fiber interacts with the molecular vibrations, due to which scattered light is generated at a wavelength longer than that of the coupled light. If another signal is also present having this longer wavelength, it undergoes amplification at the expense of the original signal. This leads to the degradation of the Signal - to - Noise Ratio (SNR) and hence the overall system performance.

2.1.1   Theory of SRS

The SRS can be viewed as modulation of light by molecular vibrations in silica matrix. This modulation produces sidebands, spaced by a frequency equal to that of the vibrating molecules, called the Stokes waves. It is explained in terms of a pump (coupled light) photon which is annihilated and a Stokes (scattered light) photon which is created along with a quantum of vibrational energy in the scattering molecules (fiber).

When high intensity pump is present, the Stokes wave grows

rapidly and a major chunk of the pump energy appears in it. The initial growth of the Stokes wave, as the pump and Stokes wave propagate along the fiber in z direction, can be described by the relation as discussed in [1].

$$\frac{dI_S}{dz} = g_R I_S I_P \qquad (2.1)$$

where

I_P = Pump intensity

I_S = Stokes intensity and

g_R = Raman Gain Coefficient

The significant feature of the Raman gain in silica fiber is that g_R extends over a large frequency range up to 40,000 GHz with a peak at 15,000 GHz, i.e., the Raman gain coefficient increases with increase in the pump-Stokes frequency separation up to a separation of about 15,000 GHz and then decreases steeply [2]. Also in case of amorphous materials, such as fused silica, the molecular vibrational frequencies spread out into bands which overlap and create a continuum. So any two copropagating light waves in silica fiber having frequency separation lying anywhere up to 40,000 GHz experience SRS effect and the extent of the effect further depends upon the value of the Raman gain coefficient at that particular frequency separation.

The effect of SRS in WDM optical fiber system is explained in detail in the following sections.

2.1.2   Power per Channel - Depletion and Amplification

A WDM system with N channels having equal channel spacing is considered here. Channels of lower wavelengths will act as pumps for the channels at the higher wavelengths which act as Stokes

14

waves. This will lead to depletion of power in some channels and amplification in others. Maximum depletion of power will occur for the channel at the lowest wavelength, i.e., the zeroth channel as it will act as the pump for the remaining N-1 channels provided the frequency separation between the zeroth and the (N-1)th channel falls within the Raman gain profile.

The fractional power lost D_0 by the zeroth channel (assuming binary 1, i.e., optical power 'ON' in each channel, scrambled polarization and Raman gain to be in linear regime) is given as [3].

$$D_0 = \sum_{i=1}^{N-1} \frac{\lambda_i}{\lambda_0} P_i \, g_{R,i} \frac{L_e}{A_e^2} \qquad (2.2)$$

where

λ_i = Wavelength of the ith channel

λ_0 = Wavelength of the zeroth channel

$g_{R,i}$ = Raman gain coefficient coupling the ith and zeroth channel

L_e = The effective fiber length given by $L_e = \frac{1}{\alpha}\left(1 - e^{-\alpha L}\right)$, where α is fiber loss coefficient and L is the fiber length

A_e = Effective core area [1], [2]. Its value is 5×10^{-7} cm^2 for a fiber core diameter of 8 μm.

P_i = The power in the ith channel.

For the calculations the Raman gain profile of the silica fiber is approximated by a triangular function, i.e., g_R rises linearly with increase in channel separation and the maximum occurs at 15,000 GHz separation and after that there is a steep fall. That is, the channels at frequency separation more than

15

15,000 GHz will not experience any SRS gain.

So,

$$g_{R,i} = \begin{cases} \dfrac{i.\Delta f}{1.5 \times 10^{13}}\, g_{Rmax} & \text{for } i.\Delta f < 15,000 \text{ GHz} \\ 0 & \text{for } i.\Delta f > 15,000 \text{ GHz} \end{cases} \qquad (2.3)$$

where Δf is the channel separation and g_{Rmax} is the peak Raman gain coefficient.

From equations (2.2) and (2.3), the fractional power loss of the jth channel due to the kth channel only, assuming equal power P for each channel, scrambled polarization and equal channel spacing Δf, is given by

$$D_{j,k} = \begin{cases} \dfrac{\lambda_k}{\lambda_j}\, P\, \dfrac{(k-j)\Delta f}{1.5 \times 10^{13}}\, g_{Rmax}\, \dfrac{L_e}{2.A_e} & \text{for } (k-j)\Delta f < 15,000 \text{ GHz and } k>j \\ 0 & \text{for } (k-j)\Delta f > 15,000 \text{ GHz} \end{cases}$$

$$(2.4)$$

where $j = 0, \ldots., (N-2)$ and

$k = 1, \ldots., (N-1)$

In Fig. 2.1, a case of four equally spaced channels is shown. An arrow labeled $D_{j,k}$ represents the fractional power loss of the jth channel due to kth channel only, where $j = 0, 1, 2$ and $k = 1, 2, 3$. Clearly at the receiver, the power in the zeroth channel will be less than the transmitted power P and the power of the channel 3 will be more than P.

Fig. 2.2 shows the depletion of power for each channel, i.e., zeroth to 29th, each having equal power and a channel separation of 4 nm, over a fiber of length 100 km and a loss coefficient $\alpha = 0.25$ dB/km. Total separation between zeroth and 29th channel is 15,000 GHz, with the zeroth channel having a wavelength of 1.55

16
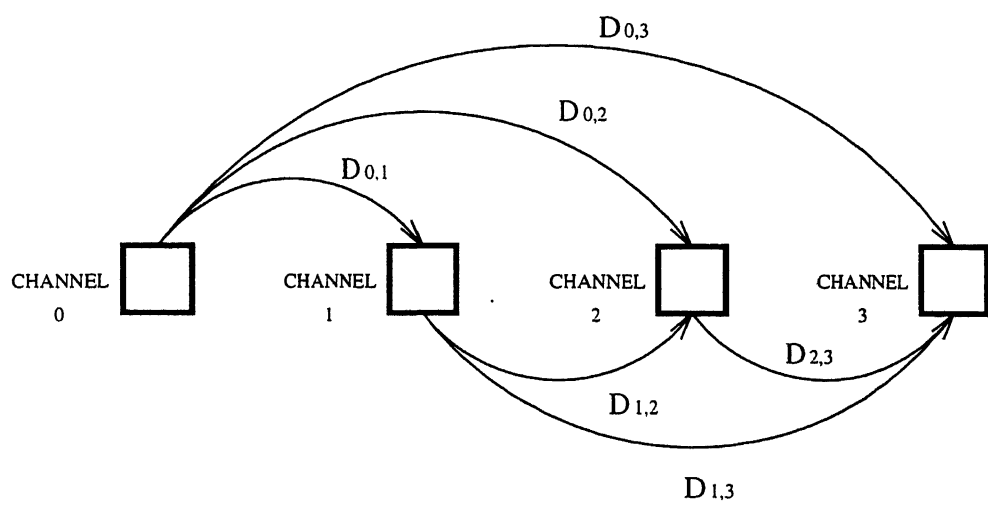
Fig. 2.1 *Diagramatic representation of power depletion and amplification due to SRS (4 channel case)*

um.   Allowable power per channel at which SNR degradation of the system is less than 0.5 dB is calculated as 716 μW, using the formula given in section 2.1.3.   The curve marked x1 in Fig. 2.2, corresponds to the case where P is equal to 1x716 μW, i.e., 716 μW.   For the curve marked x2, P =2x716 μW, and so on.   Fig. 2.2 shows that the depletion, i.e., fractional power loss is maximum for the zeroth channel and zero for the 29th channel.   Also the depletion increases with increase in the power per channel.

Fig. 2.3 shows the modified power per channel at the receiver due to the SRS effect.   For the channels in the first half, i.e., zeroth to 13th channels, there is a depletion of power, where as for the channels in the second half, there is amplification.   Also the channel in the middle (number 14) has almost the same power as transmitted.   Three cases with different transmitted power are considered.   In the case indicated by x4, where power per channel is 4 times the allowable power per channel, the difference among the power of zeroth and 29th channel is the largest.

2.1.3   **SNR Degradation**

As discussed previously, that the worst affected channel, i.e., the lowest wavelength channel, in the WDM system loses the most in terms of power depletion.   So at the receiver this channel suffers the most in terms of SNR degradation.   SNR degradation is related to the power depletion D_O of the worst effected channel as

$$SNR \_ degradation = -10 \log (1-D_O) \qquad (2.5)$$

SNR _ degradation up to 0.5dB is tolerable in practical systems.

Channel separation = 4nm, 100 km system

Channels with allowable power/ch. x times =

— x1
--- x2
--- x4
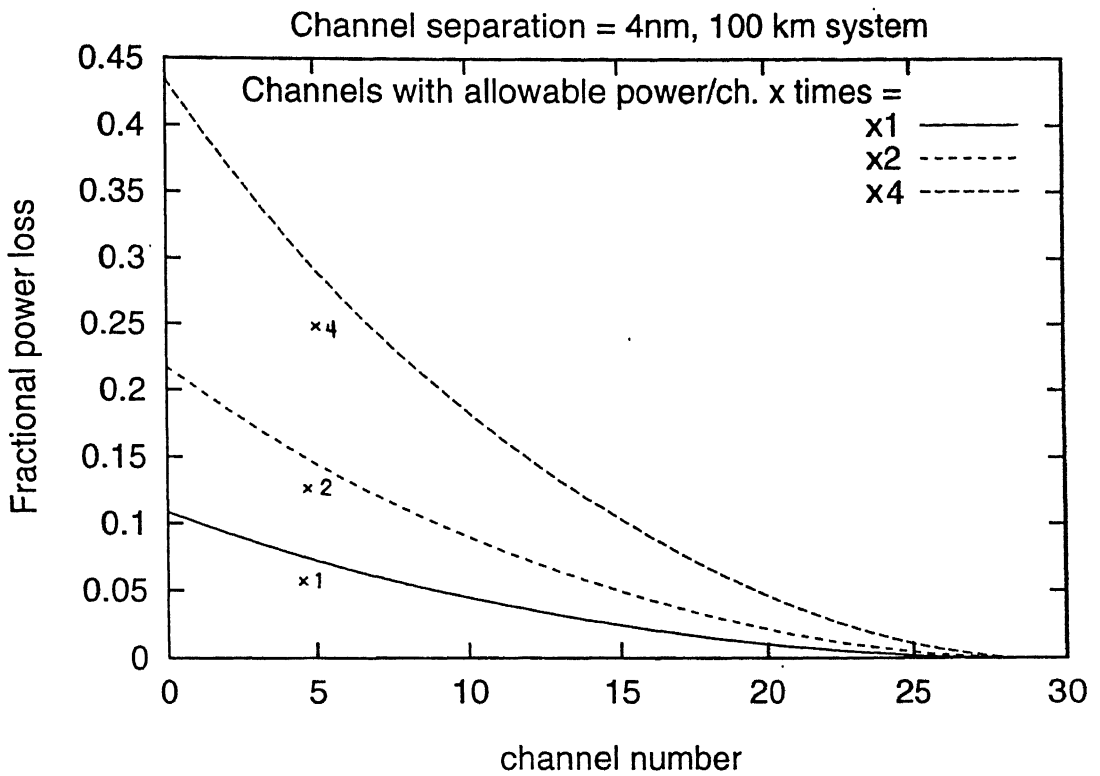
Fig. 2.2 Fractional power loss per channel due to SRS

Channel separation = 4nm, 100 km system

Channels with allowable power/ch. x times =

— x1
--- x2
--- x4
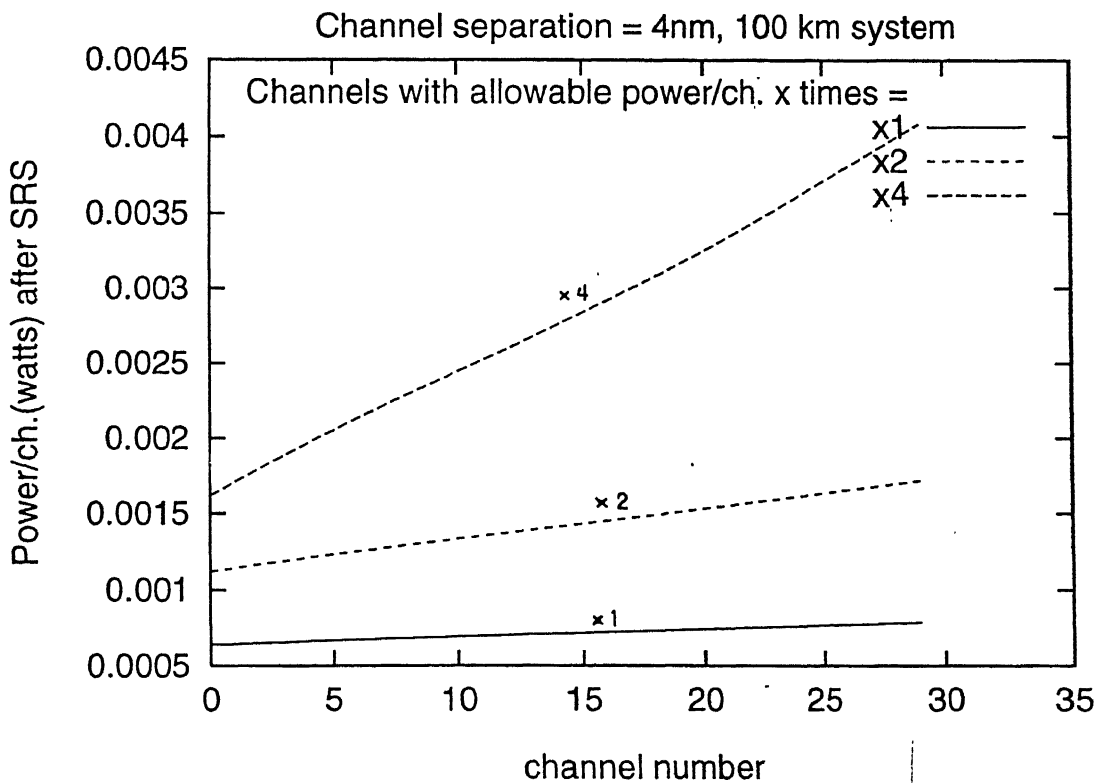
Fig. 2.3 Modified power per channel due to SRS

2.1.4   Limit on Power Per Channel

In section 2.1.2 it was observed that the depletion of power is proportional to the transmitted power per channel. Also in section 2.1.3 the power depletion is related to the SNR degradation. So to keep the SNR degradation less than 0.5 dB, a limit is imposed on the maximum power to be transmitted in each channel.

Case 1 : When all the N channels with equal channel separation Δf fall within the Raman gain profile.

Using equations (2.2) and (2.3),

$$D_o = \frac{\Delta f \; g_{Rmax} P \; L_e \; N \; (N-1)}{A_e \; 6 \times 10^{13}} \qquad (2.6)$$

and using equations (2.5) and (2.6) for power depletion less than 0.5 dB, the upper bound on power per channel is obtained as

$$\text{Maximum power per channel} < \frac{6.522 \times 10^7 \; A_e \alpha}{g_{Rmax} \; \Delta f \; (N-1) N (1 - e^{-\alpha L})} \qquad (2.7)$$

where L is the fiber length in km

A_e is effective area in cm^2

$$g_{Rmax} = \left(\frac{9.4 \times 10^{-18}}{\lambda_o} \right) \; cm/W$$

λ_o is the wavelength of the zeroth channel in meters

Case 2 : When out of the N channels only, $J = (15 \times 10^{12}/\Delta f)$ channels fall within the Raman gain profile.

For $J \gg 1$ so that $(J-1) \approx J$, using equations (2.2), (2.3) and (2.5), we have

$$\text{Maximum power per channel} < \frac{2.9 \times 10^{-19} \; A_e \; \Delta f \; \alpha}{g_{Rmax} (1 - e^{-\alpha L})} \qquad (2.8)$$

In case of systems with inline amplification, the overall

20

effective length is given by the sum of the effective lengths of the amplified segments.

So the expressions (2.7) and (2.8) are modified for the system with M inline amplifiers as

Maximum power per channel $< \dfrac{6.522\text{x}10^{7}\ A_e\alpha}{g_{Rmax}\ \Delta f\ (N-1)\ N\ (M+1)\ (1-e^{-\alpha La})}$

$$(2.9)\ \text{(Case 1)}$$

and

Maximum power per channel $< \dfrac{2.9\text{x}10^{-19}\ A_e\Delta f\ \alpha}{g_{Rmax}\ (M+1)\ (1-e^{-\alpha La})}$

$$(2.10)\ \text{(Case 2)}$$

where La is length of each amplified segment in km.

From the above expressions it is clear that the power limit per channel imposed by SRS depends on

- the number of channels,
- the channel separation, and
- the amplifier separation, i.e., length of each amplified segment

In Figs. 2.4 and 2.6, for 4 nm channel separation, the maximum allowable power per channel after 30 channels is constant. It is due to the fact that with a 4 nm channel separation, only 30 channels fall within the Raman gain profile. So as indicated by equations (2.8) and (2.10), when all the channels do not fall within the Raman gain profile, but the number of channels falling within the profile is much greater than 1, the power limit is independent of the number of channels.

Figs. 2.4 and 2.5 show that for smaller amplified segment lengths, over the same overall system length and channel numbers,
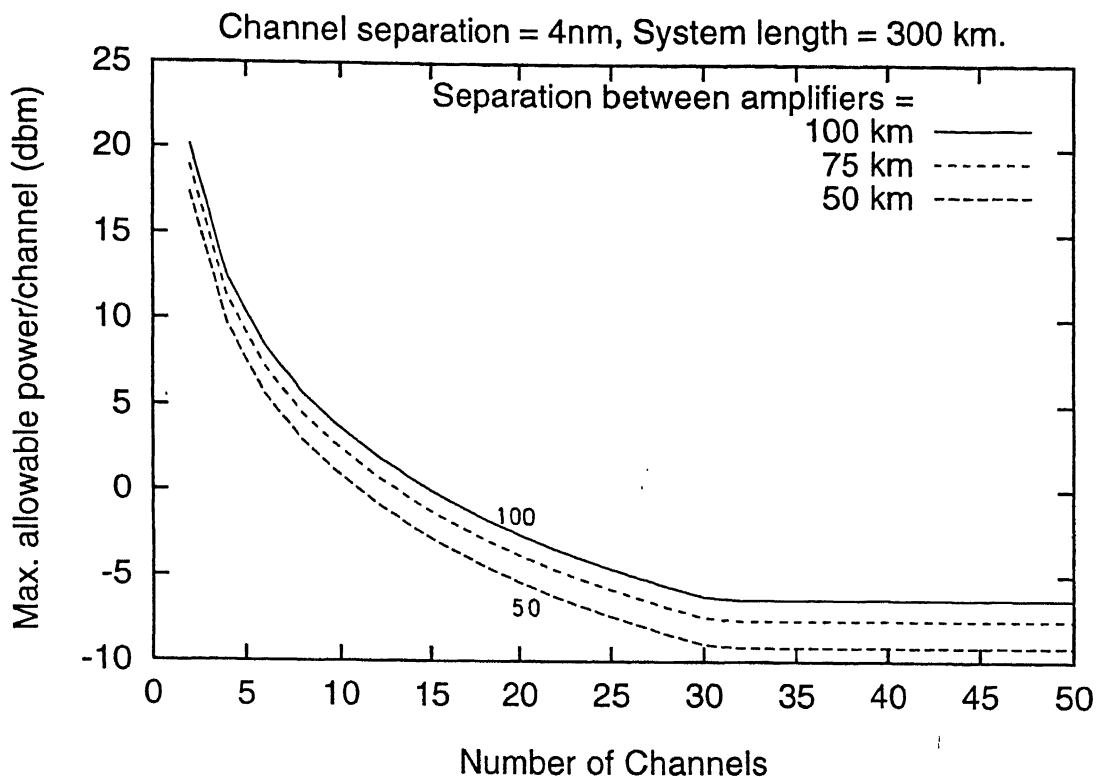
Channel separation = 4nm, System length = 300 km.

Fig. 2.4 Limit on power per channel due to SRS Vs number of channels for different amplifier spacings

Channel separation = 4nm, 4 Channels
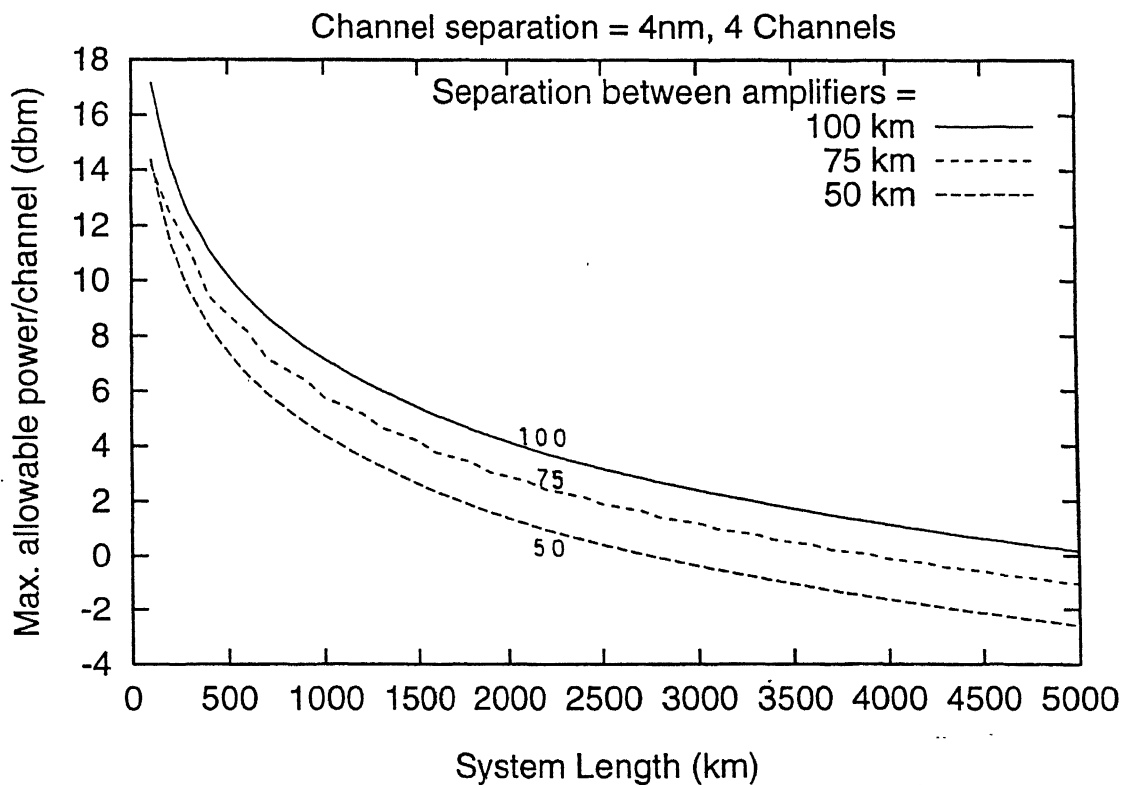
Fig. 2.5 Limit on power per channel due to SRS Vs system length for different amplifier spacings
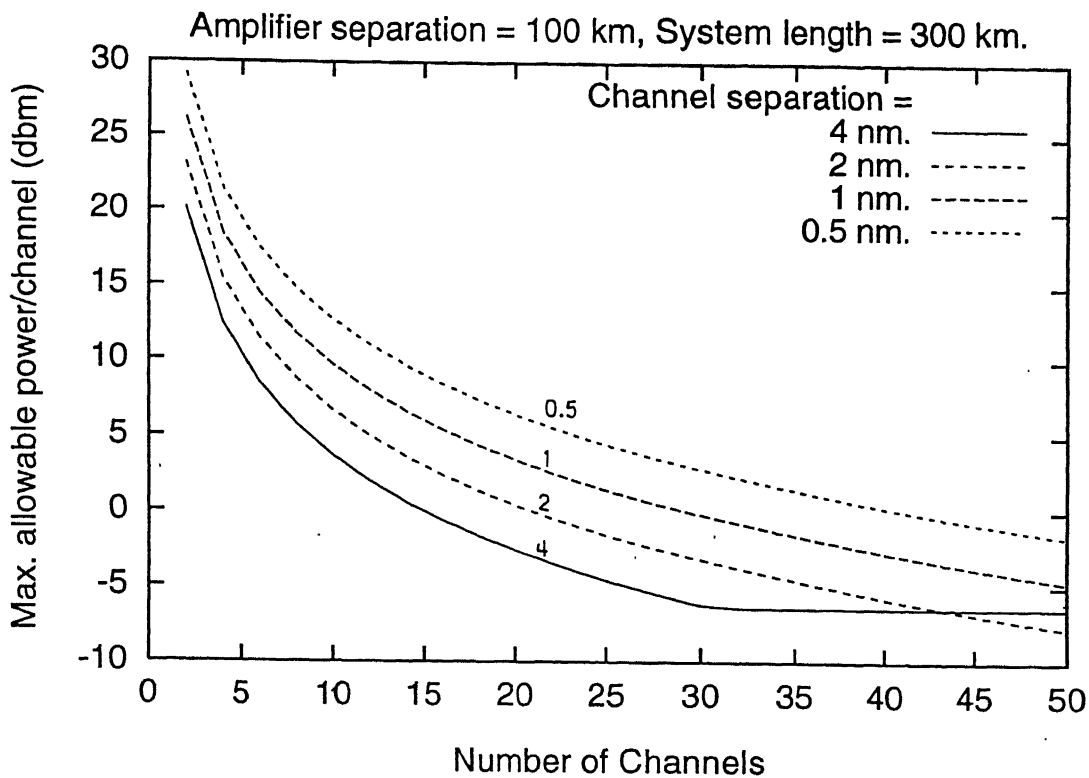
Fig. 2.6 Limit on power per channel due to SRS Vs number of channels for different channel separations
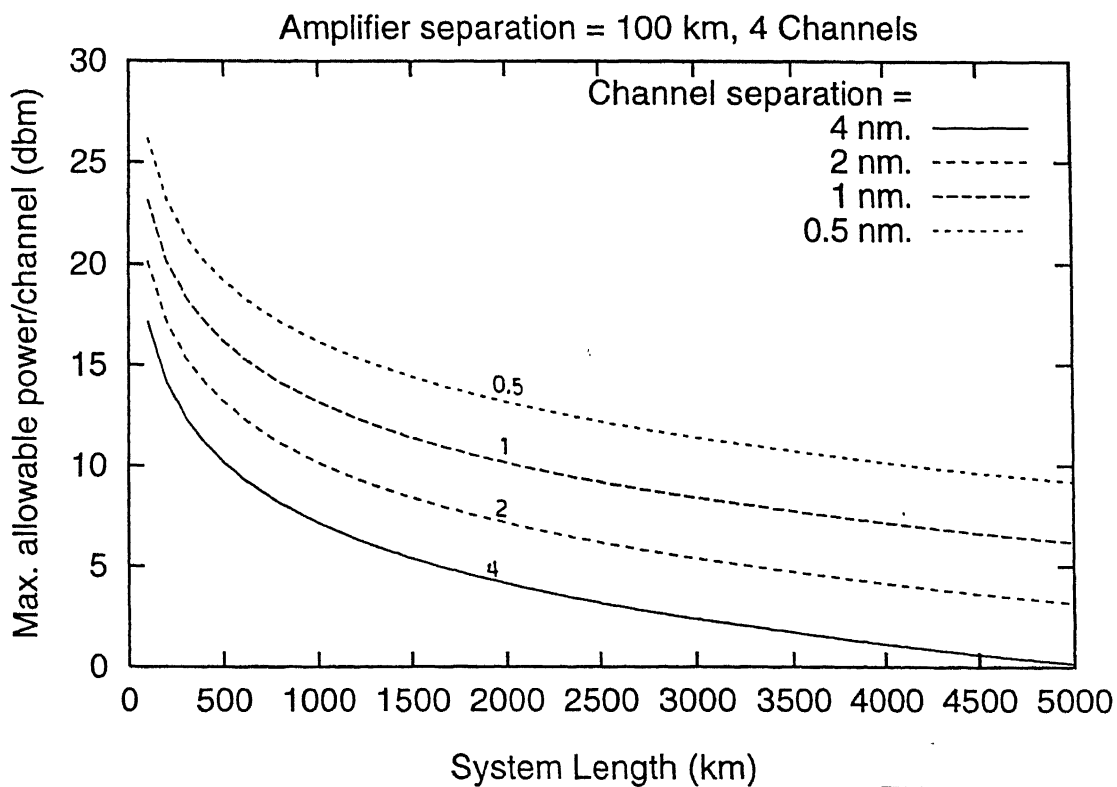
Fig. 2.7 Limit on power per channel due to SRS Vs system length for different channel separations

the effect of SRS is more, thus the power per channel becomes less. This is due to the fact that for smaller amplified segments, the overall effective length of the system, over the same system length, increases.

Figs. 2.6 and 2.7 indicate that the SRS effect is more severe for higher channel separation.

2.2 FOUR WAVE MIXING (FWM)

In the SRS effect discussed in section 2.1, the optical fiber played an active role through the participation of molecular vibrations. But in the case of FWM, optical fiber plays a passive role, i.e., it simply mediates the interaction among several copropagating optical signals.

2.2.1 Theory of FWM

In the case of the WDM systems, a number of optical waves copropagate at different wavelengths. Because of the FWM effect, three copropagating optical signals of frequencies say f_i, f_j and f_k interact and generate a fourth signal at frequency f_{ijk}, where $f_{ijk} = f_i + f_j - f_k$. So in WDM systems many such signals copropagate with the original signals and grow at their expense. This phenomenon is known as FWM and is due to nonlinear response of a dielectric medium (optical fiber) to the intense light (WDM signal) [1].

These newly generated signals can interfere with the original signals if there happens to be some frequency match between them, which leads to crosstalk and degradation of the system performance. Probability of this frequency match increases if the channels are equally spaced. Effect of FWM is even more severe in

24

the systems with inline amplification, as due to inline amplification the effective length of the fiber, over which nonlinear interaction takes place, increases.

FWM power at newly generated frequency f_{ijk} is given by [4], [5].

$$P\left(f_{ijk} = f_i + f_j - f_k\right) = k^2 P_i P_j P_k \, e^{-\alpha L}\left(\frac{L_e}{A_e}\right)^2 \eta_{ijk} \, d^2_{ijk} \qquad (2.11)$$

where

$$k = \frac{32\pi^3 \chi_{1111}}{n^2 \, c \, \lambda} \text{ and } L_e = \frac{1}{\alpha}\left(1 - e^{-\alpha L}\right)$$

n is refractive index of the fiber

λ is centre wavelength

L is system length

A_e is effective area of fiber

d_{ijk} is degeneracy factor. Its value is 3 (for i=j) and 6 (for i≠j)

χ_{1111} is third order nonlinear electric susceptibility (5×10^{-14} esu)

η_{ijk} is FWM efficiency which is given by

$$\eta_{ijk} = \left(\frac{\alpha^2}{\alpha^2 + \Delta\beta^2_{ijk}}\right)\left[1 + \frac{4e^{-\alpha L}}{(1 - e^{-\alpha L})^2} \sin^2\left(\Delta\beta_{ijk} \frac{L}{2}\right)\right] \qquad (2.12)$$

P_i, P_j and P_k represent power in the ith, jth and kth channels, respectively.

$\Delta\beta_{ijk}$ is phase mismatch among the channels i, j and k. Its value depends on channel separation and fiber dispersion coefficient [4]. It is expressed as

25

$$\Delta\beta_{ijk} = \left[\frac{2\pi\lambda^2}{c}\right]\left(|f_i - f_k| \cdot |f_j - f_k|\right) \cdot \left\{D + \frac{dD}{d\lambda}\left[\frac{\lambda^2}{2c}\right]\right.$$

$$\left. \cdot \left(|f_i - f_k| + |f_j - f_k|\right)\right\} \qquad (2.13)$$

In a WDM system with M inline amplifiers, during the worst case when the generated FWM signals in each amplified segments of length La are added in phase at the receiver side of the link, the total effective length increases by (M+1) times as compared to the case with no inline amplifiers.

So FWM power generated at frequency f_{ijk} in this case, i.e., with inline amplifiers, is (assuming equal signal power P in every channel).

$$P\left(f_{ijk}\right) = k^2 P^3 \ e^{-\alpha La} \left[\frac{(M+1) \ L_e}{A_e}\right]^2 \eta_{ijk} \ d_{ijk}^2 \qquad (2.14)$$

Total FWM power generated at frequency f_{ijk} is

$$P_T\left(f_{ijk}\right) = \sum_{f_{ijk} = f_i + f_j - f_k} P\left(f_{ijk}\right)$$

$$= k^2 \ P^3 \ e^{-\alpha La} \left[\frac{(M+1) \ L_e}{A_e}\right]^2 \sum_{f_{ijk} = f_i + f_j - f_k} \eta_{ijk} \ d_{ijk}^2 \qquad (2.15)$$

Summation is made over all relevant combinations satisfying the relationship $f_{ijk} = f_i + f_j - f_k$ in the WDM system with N channels.

2.2.2   FWM Limit on Power Per Channel

From equation (2.15) it is clear that the total FWM noise power at a particular frequency is proportional to cube of the power per channel. So FWM noise tolerance of the receiver imposes a limit on power per channel.

26

The optical SNR due to FWM noise only at the receiver is given by

$$\frac{S}{FWM\_Noise} = \frac{P \, e^{-\alpha La}}{P_T(f_{ijk})} \tag{2.16}$$

Using equation (2.15) and (2.16)

$$\frac{FWM\_Noise}{S} = k^2 P^2 \left[\frac{(M+1) \, L_e}{A_e}\right]^2 \sum \eta_{ijk} \, d_{ijk}^2$$
$$f_{ijk} = f_i + f_j - f_k$$

Therefore,

$$P = \left[\frac{A_e}{(M+1) \, L_e}\right] \left[\sqrt{\frac{1}{\left(S/FWM\_Noise\right) k^2 \sum \eta_{ijk} \, d_{ijk}^2}}\right]$$
$$f_{ijk} = f_i + f_j - f_k$$

$$(2.17)$$

For the worst affected channel out of N channels, value of $\sum \eta_{ijk} \, d_{ijk}^2$ will be the maximum. So

Maximum allowable power per channel

$$= \min_{ijk \, = \, 1 \text{ to } N} \left\{\left[\frac{A_e}{(M+1) \, L_e}\right] \left[\sqrt{\frac{1}{\left(S/FWM\_Noise\right) k^2 \sum \eta_{ijk} \, d_{ijk}^2}}\right]\right.$$
$$f_{ijk} = f_i + f_j - f_k$$

$$(2.18)$$

Effects due to changes in the number of channels, channel separation, fiber chromatic dispersion and amplifier spacing, on the maximum allowable power per channel is discussed in the following sections.

2.2.2.1 Effect of Number of Channels

In case of equally spaced channels, the worst affected channel is the one at the centre, and also the FWM efficiency depends on the separation of the interacting channels (equations

.12 and 2.13). So the major part of FWM noise is generated by the interaction of the channels which are in close neighbourhood of the worst affected channel. Also, with increase in the number of channels there is not much increase in the number of the close neighbourhood members beyond a certain limit. Due to this in Figs. 2.9 and 2.11, it can be seen that, there is a sharp drop near N = 5, but, after that allowable power per channel remains almost constant with increase in the number of channels.

For the Figs. 2.8 to 2.11, fiber chromatic dispersion coefficient D = 2 ps/nm-km and $dD/d\lambda$ = 0.09 ps/km-nm^2.

.2.2.2 *Effect of Channel Separation*

In Figs. 2.10 and 2.11, four cases of different channel separations are considered. Allowable power per channel decreases with decrease in channel separation as the FWM efficiency increases (equations 2.12 and 2.13).

.2.2.3 *Effect of Amplifier Spacing*

Figs. 2.8 and 2.9 shows that with decrease in amplifier spacing FWM effect becomes more severe. The reason for this is that for the given system length when amplifier spacing is decreased, the number of amplified segments increases, on the other hand, decrease in effective length per segment is not that much. So the overall effective length increases, which in turn increases the FWM noise power (equation 2.15).

.2.2.4 *Effect of Fiber Chromatic Dispersion*

It is seen in Fig. 2.12 that with increasing fiber chromatic dispersion coefficient D, the effect of FWM reduces. But increase in D leads to other dispersion related problems which will be more
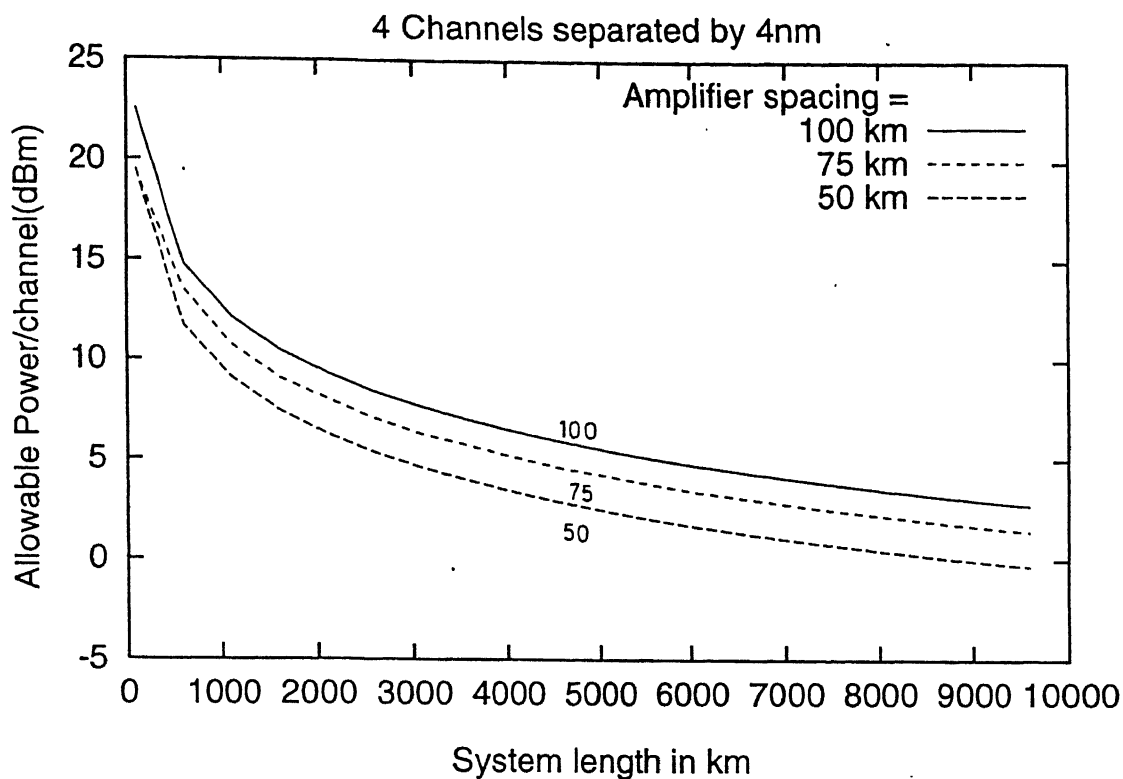
4 Channels separated by 4nm

Amplifier spacing =
100 km ———
75 km - - - - -
50 km - - - - -

Allowable Power/channel(dBm)

100

75

50

System length in km

Fig. 2.8 Limit on power per channel due to FWM Vs system length for different amplifier spacings

System Length = 300km, Channel Separation = 4nm

Amplifier spacing =
100 km ———
75 km - - - - -
50 km - - - - -

Allowable Power/channel(dBm)

100

75

50

Number of channels

Fig. 2.9 Limit on power per channel due to FWM Vs number of channels for different amplifier spacing
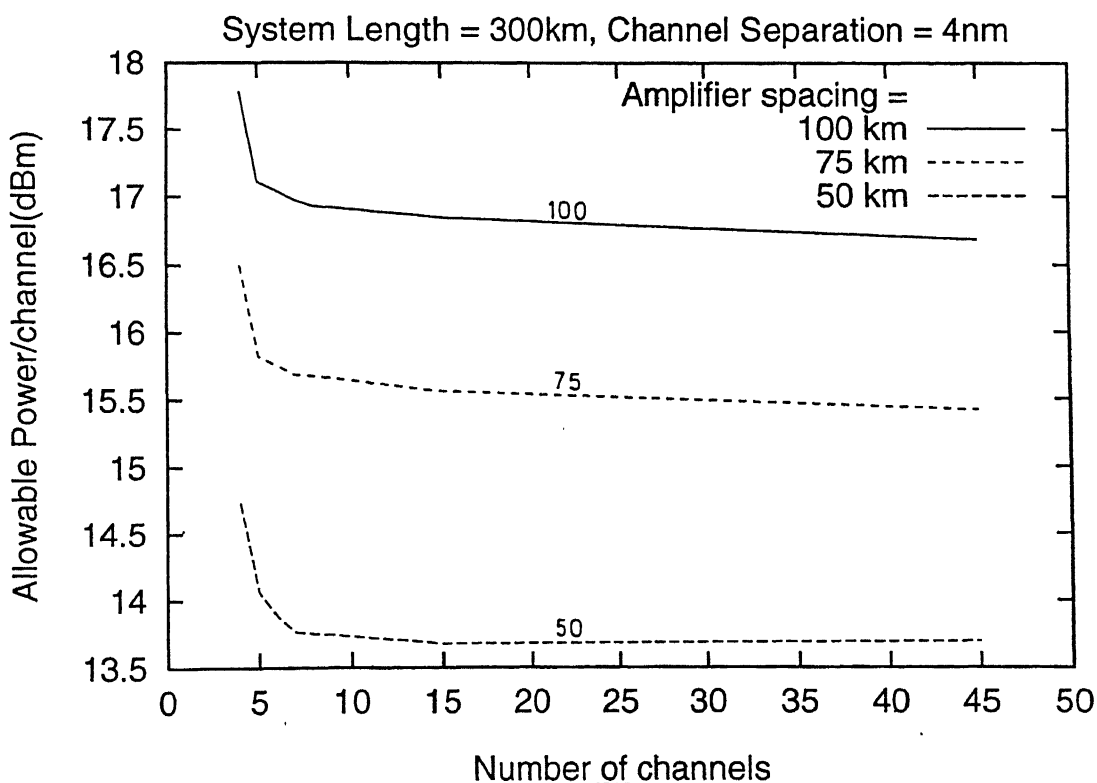
4 Channels, Amplifier spacing = 100km
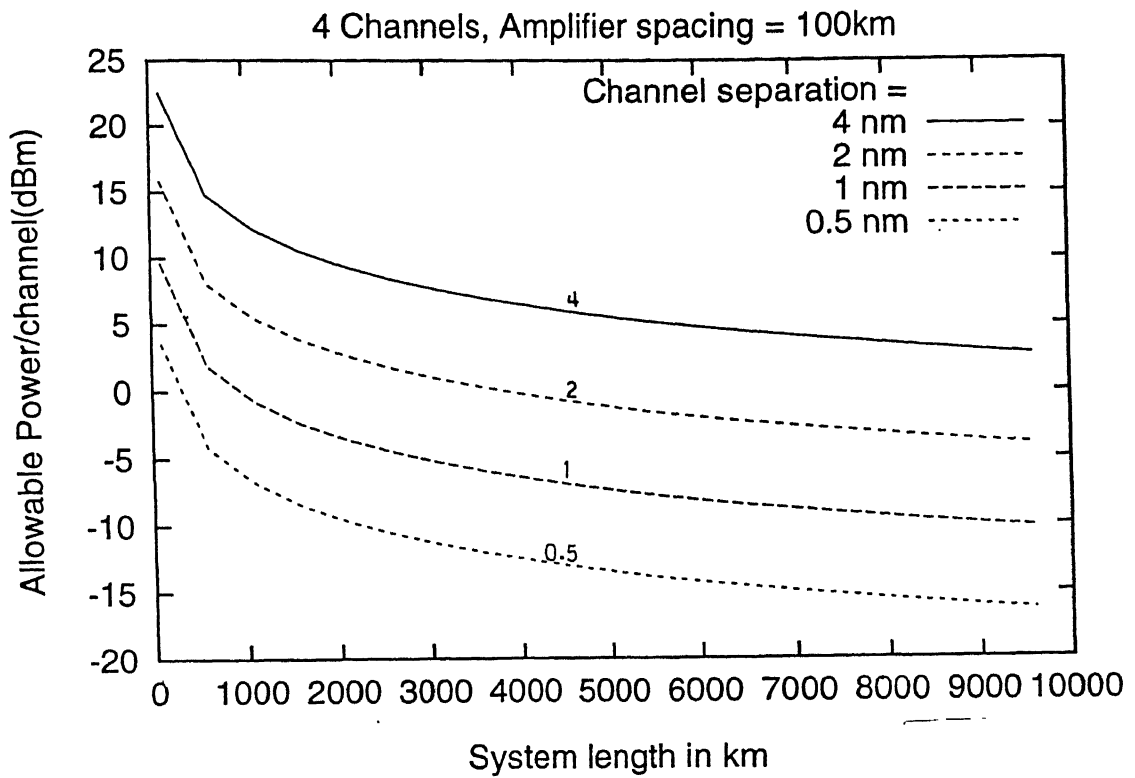
Fig. 2.10 Limit on power per channel due to FWM Vs system length for different channel separations

System Length = 300km, Amplifier spacing = 100km
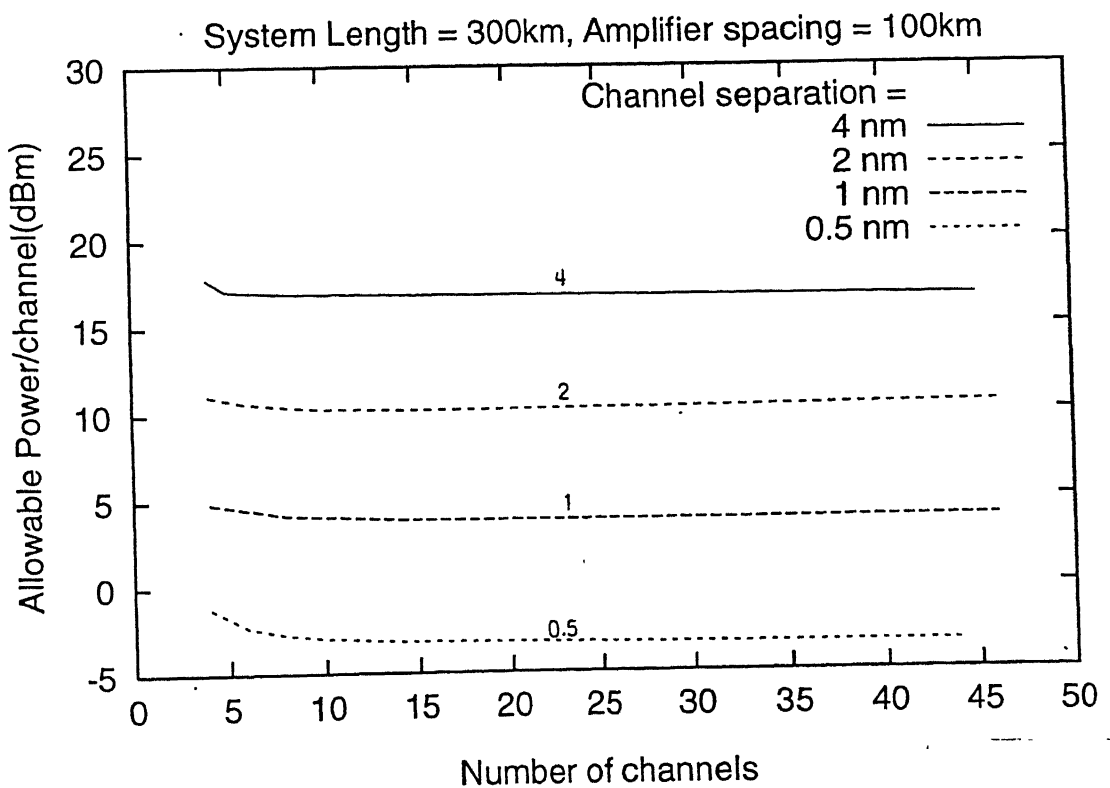
Fig. 2.11 Limit on power per channel due to FWM Vs number of channels for different channel separation:
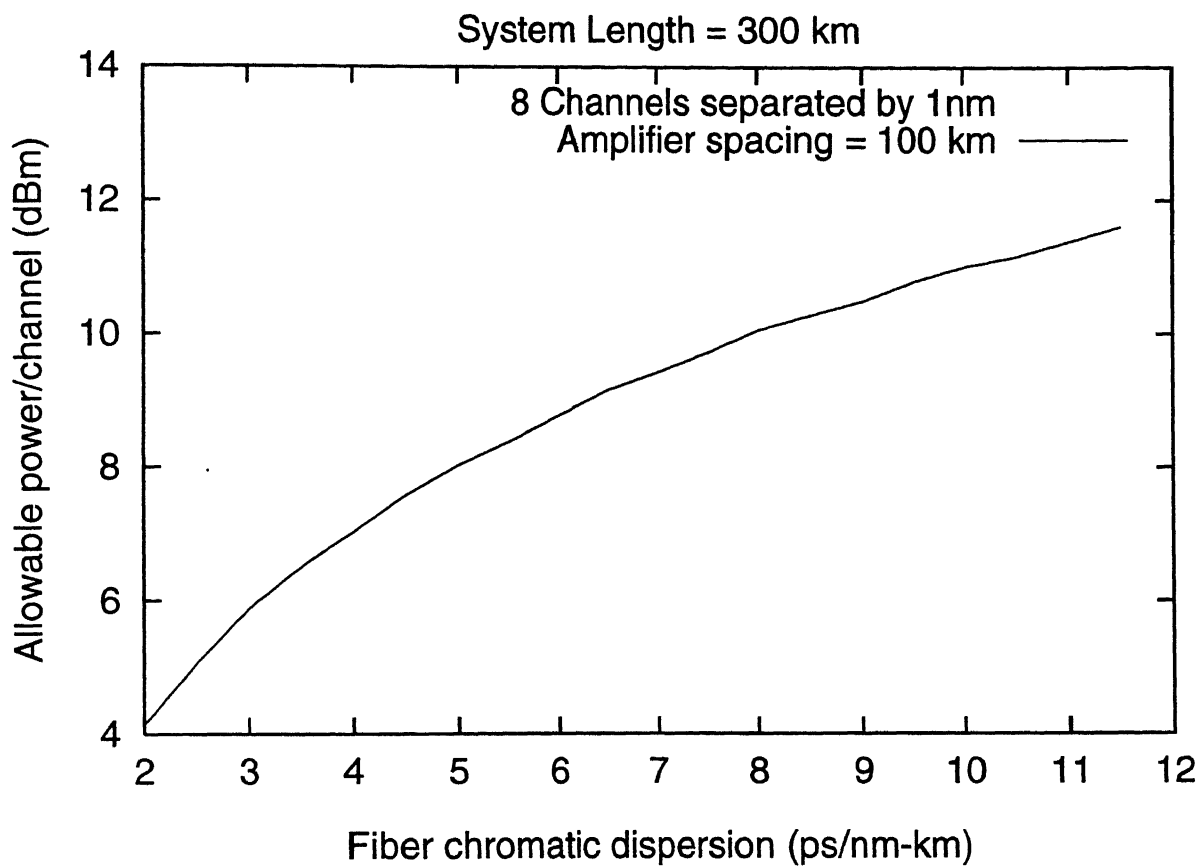
Fig. 2.12 Maximum allowable power per channel Vs fiber chromatic dispersion coefficient

31

armful to system performance. So dispersion is kept at the inimum and FWM is controlled by adjusting the channel separation epending upon the system requirements.

It is observed in sections 2.1 and 2.2, that channel eparation has opposite effect on SRS and FWM. So while designing n efficient WDM system some optimisation of channel separation is equired to keep both FWM and SRS effects at the minimum.

CHAPTER - 3
PROBLEMS INDUCED DUE TO INLINE AMPLIFICATION

The use of inline optical amplifiers has extended the optical network dimensions to thousands of kilometers and made the concept of transparent optical network quite feasible. But their use introduces problems like accumulation of Amplified Spontaneous Emission (ASE) noise and aggravation of fiber nonlinearity effects like SRS and FWM. The aggravation of FWM and SRS effects has already been discussed in the previous chapter. In this chapter accumulation of ASE noise is considered.

3.1 TYPICAL CHARACTERISTICS OF EDFA

In a WDM optical fiber system, for inline amplification, Erabium Doped Fiber Amplifier (EDFA) is perferred to semiconductor laser Amplifier (SLA) because of the following typical characteristics of an EDFA [6]

■ High Gain : EDFA provides high gain (30-50dB) in 1.55 μm band

■ High output : EDFA is capable of delivering 10 to 20 dBm of optical power into a fiber

■ Noise : Noise figure is quite low, i.e, 3 to 5 dB

■ Bandwidth : It provides a large bandwidth, several hundred GHz to THz, which is an important factor when an EDFA is used as a multi wavelength common amplifier in WDM systems.

Also the variation of the gain resulting from temperature change and ageing is less significant in an EDFA than in a SLA. Due to the above mentioned characteristics, an EDFA is a better choice for inline amplification in WDM optical fiber systems.

3.2 SIMPLE AMPLIFIER MODEL

A simple model of a saturating EDFA, given in [7], is considered here. The long transient response time of gain saturation in EDFAs enable them to operate saturated in gigabit-per-second systems without causing any crosstalk penalties [7], [8]. Also for the saturated amplifiers good conversion efficiency of a pump power into signal power is achieved [7].

As mentioned in [7], two possibilities, i.e, keeping the total power at the output of each amplifier constant throughout the cascaded amplifier system shown in fig. 3.1 or keeping the signal power at the output of each amplifier constant, are considered.

In the fig. 3.1,

L_a is length of an amplified segment

EDFA is an Erbium Doped Fiber Amplifier

I is an Isolator used to prevent the backward propagation of the
ASE noise

$P_{s,o}$ is Initial optical power coupled into the fiber

P_{ase} is ASE noise power contribution of one amplifier

$P_{T,i}$ is total optical power of the output of the ith amplifier,
where i = 1, 2, ..., M

$P_{s,i}$ is signal power of the output of the ith amplifier for i = 1,
2, ..., M

3.2.1 Constant Total Output Power

In this case the total output power at the output of each amplifier is kept constant, i.e, $P_{T,i} = P_{s,o}$, i = 1,....,M, by adjusting the gain of each amplifier to compensate for the loss occured due to fiber attention in the previous segment and connector losses.

$P_{T,1} = P_{ase} + P_{S,1}$ $P_{T,2} = 2 P_{ase} + P_{S,2}$ $P_{T,M} = M P_{ase} + P$
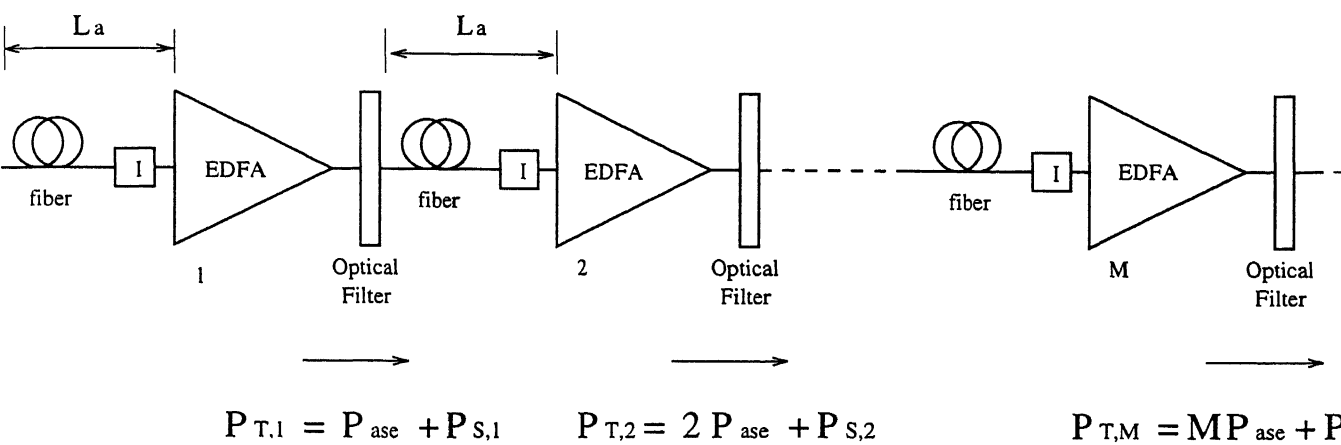
Fig. 3.1   *Cascaded amplifier system showing accumulation of ASE noise*

The gain of each amplifier stage is given as [7]

$$G = \frac{P_{s,o} + 2N_{sp} \, \nu hB_o}{2N_{sp} \nu hB_o + A.P_{s,o}} \qquad (3.1)$$

where

N_{sp} is spontaneous emission noise factor (assumed constant, 1.3, for each amplifier)

h is Plank's constant (6.63×10^{-34} J.S)

B_o is filter bandwidth in each stage

A is loss over the fiber length 'La' (km) + connector loss

From (3.1) in the limit $2N_{sp}h\nu B_o < < P_{s,o}$

$$G = \frac{1}{A}$$

Also $P_{sat} = \frac{(1-A).P_{s,o}}{\ln(AG_o)}$

where

P_{sat} is Saturation power of each amplifier

G_o is Unsaturated gain of each amplifier

3.2.1.1 *Maximum Achievable System Length (Ideal Filtering)*

As the amplifier stages are traversed, the ASE noise keeps on accumulating and consequently the signal power decreases to keep the total power at the output of each amplifier constant. Difficulty of increasing the amplifier saturation power beyond the present limit (about +15 dbm) [9], poses a constraint on the increase of $P_{s,o}$ and hence limits the maximum achievable system length for a given ratio of signal power to ASE noise power (P_s/P_{ase}). Fig. 3.2 gives the maximum achievable system length for $P_s/P_{ase} = 1$ in terms of amplified segments, of about 3500 km for $P_{total} \approx 0.035$ W, fiber attenuation constant $\alpha = 0.25$ dB/km, connector losses per amplified segment = 5 dB, and data rate - per - channel = 2.5 Gbits/sec (assuming that there is no reduction in the end-to-end bandwidth of the system due to cascading of the

filters).

3.2.1.2 *Maximum Achievable System Length (Nonideal Filtering)*

At the output of each EDFA an optical filter is used to reject the ASE noise outside the signal band. Filters used in the system are interference type. Due to cascading of M such filters, the end-to-end bandwidth is reduced by $\left(\frac{\ln 2}{M}\right)^{1/6}$, [7].

The reduction of end-to-end bandwidth due to cascading of interference filters is least compared to the reduction due to Grating type or Fabry - Perot type filters [9]. Because of this, bandwidth of each filter is increased accordingly so that the reduced end-to-end bandwidth is sufficient to accommodate the WDM signal. This increase in the bandwidth of each filter enhances the amount of ASE noise power contributed by each amplifier, which in turn decreases the maximum achievable system length for a given (P_s/P_{ase}) ratio.

Fig. 3.3 shows that the maximum achievable system length in this case is reduced to almost a half of the system length achieved in ideal filtering case under the similar conditions.

3.2.2 Constant Output Signal Power

In this case the signal power at the output of each amplifier is kept constant, i.e, $P_{s,i} = P_{s,o}$ for $i = 1, \ldots, M$ [7].

Here

$$P_{T,i} = P_{s,o} + i\, 2\, N_{sp}(G - 1)\, h\, \nu\, B_o \qquad (3.3)$$

$$P_{sat} = \frac{1 - A}{\ln(AG_o)}\left(P_{s,o} + i\, 2N_{sp}\, (G-1)\, h\, \nu\, B_o\right) \qquad (3.4)$$

$$G_i = \frac{1}{A} \qquad (3.5)$$

for $i = 1, 2, \ldots, M$

3.2.2.1 *Maximum Achievable System Length (Ideal Filtering)*

The saturation power of each successive amplifier is increased slightly to compensate for the gain saturation caused by

Constant Ptotal (Ideal case)

4 channels separated by 4nm.

Psignal ———
Ptotal - - - - -
Pase noise - - - - - -

Ptotal

Optical Power (watts)

Amplified Segments(100 kms. each)
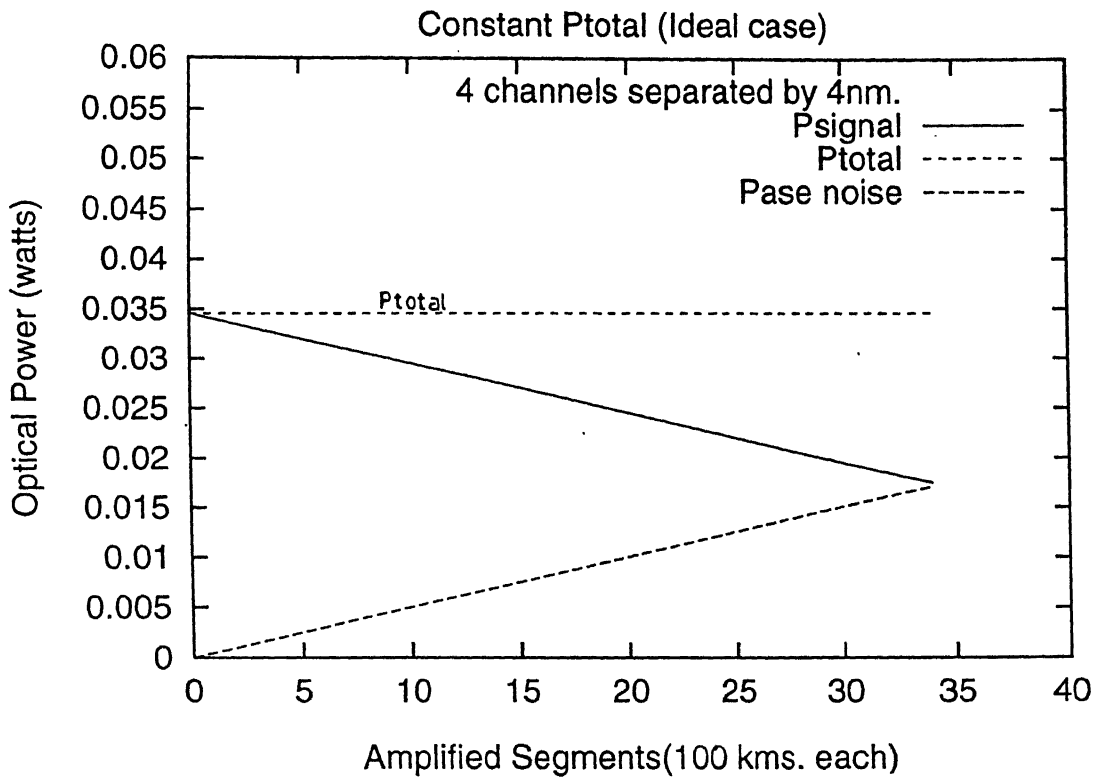
Fig. 3.2 Ptotal, Psignal, Pase_noise Vs system length for constant Ptotal and ideal filtering

Effect of cascaded filters included

4 channels separated by 4nm.

Psignal ———
Ptotal - - - - -
Pase noise - - - - - -

Ptotal

Optical Power (watts)

Amplified Segments(100 kms. each)
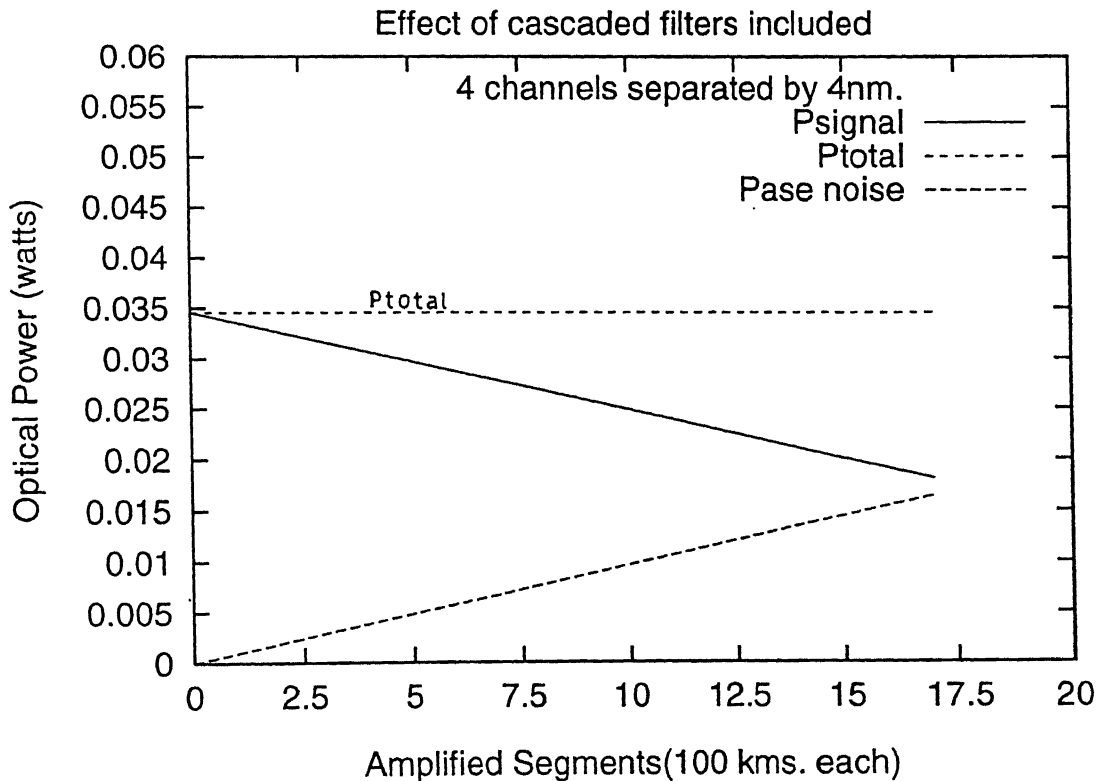
Fig. 3.3 Ptotal, Psignal, Pase_noise Vs system length for constant Ptotal and nonideal filtering

the buildup of the ASE noise. The upper bound on the saturation power imposes limit on the initial power coupled to the fiber and hence limits the maximum attainable system length for a given P_s/P_{ase} ratio. Fig. 3.4 shows this system length which is almost equal to the length attained using the constant total output power case under similar conditions.

3.2.2.2 *Maximum Achievable System Length (Nonideal Filtering)*

Here again because of the reduction of end-to-end bandwidth due to cascaded filters, the maximum achievable system length is reduced to almost half the length which was achieved in the ideal filtering case, Fig. 3.5.

3.2.3 Accumulation of ASE Noise

ASE noise introduced by an amplifier is proportional to the gain of the amplifier. The gain is adjusted to compensate for the fiber loss + connector loss in an amplified segment. So variation in amplifier separation (length of amplified segment) varies the amount of the ASE noise introduced by the amplifier. For smaller amplifier separation the gain required for each amplifier decreases which inturn decreases the amount of the ASE noise introduced. Fig. 3.6 shows the increase in the ASE noise power with amplifier stages for different amplifier separations, i.e., 100 km, 75 km and 50 km.

It is observed here (and also in chapter 2) that a decrease in amplifier separation has opposite effects on noise generated due to the fiber nonlinearities (SRS and FWM) and ASE noise accumulation. Whereas the ASE noise reduces in such a case, the SRS and FWM effects increase.

In the next chapter effects of SRS and FWM for determining the maximum achievable system length for a given P_s/P_{ase} ratio will be discussed.

Constant signal power (Ideal case)

4 channels separated by 4nm.

Psignal ——————
Ptotal ------------
Pase noise ------------

Ptotal

Optical power out from amplifier(watts)

Amplified Segments(100 kms. each)
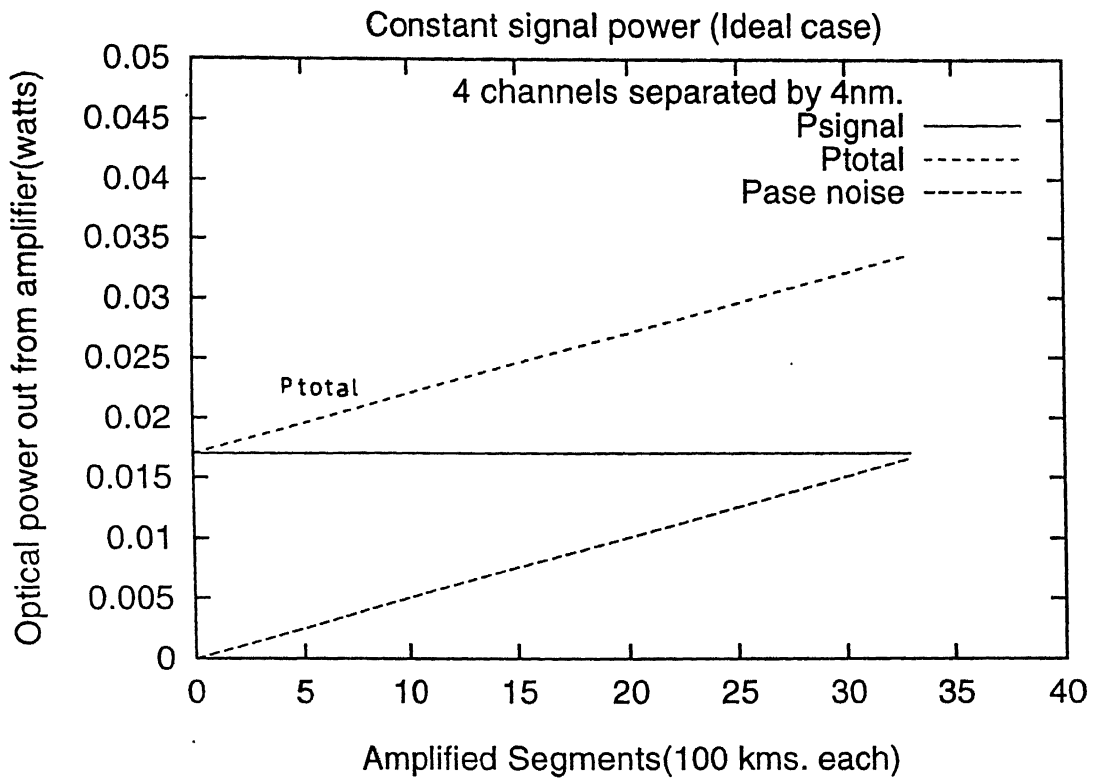
Fig . 3.4 Ptotal, Psignal, Pase_noise Vs system length for constant Psignal and ideal filtering

Effect of cascaded filters included

4 channels separated by 4nm.

Psignal ——————
Ptotal ------------
Pase noise ------------

Ptotal

Optical Power out from amplfier(watts)

Amplified Segments(100 kms. each)
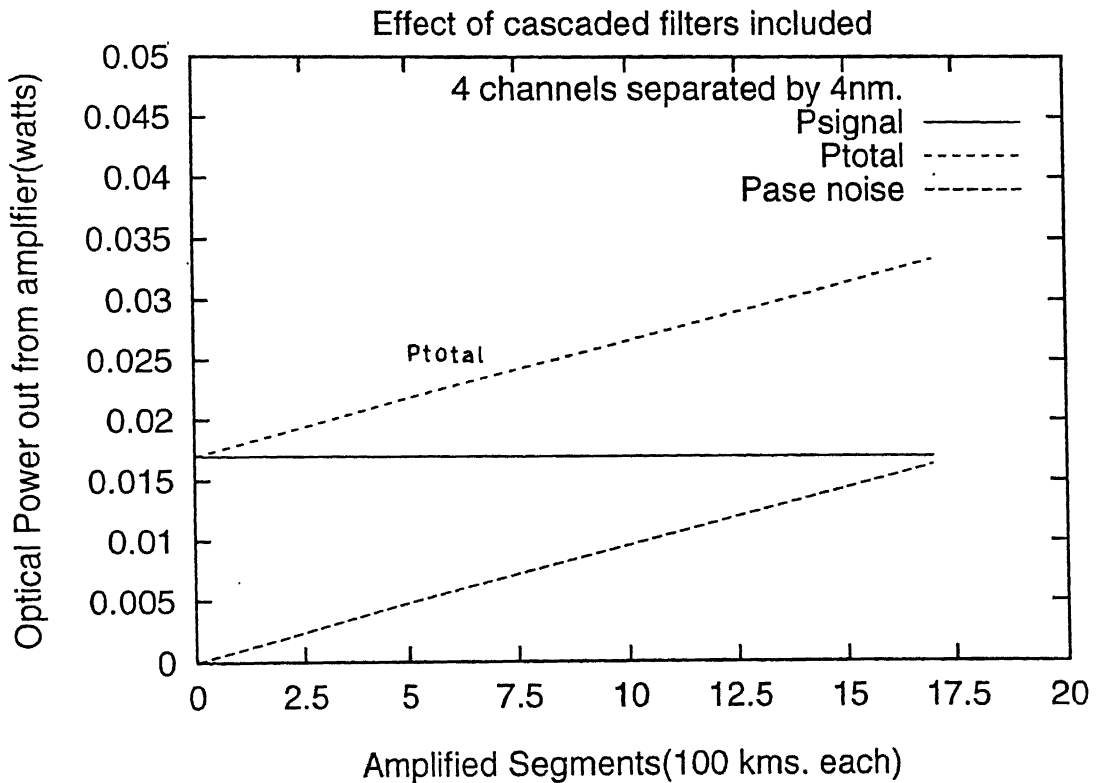
Fig. 3.5 Ptotal, Psignal, Pase_noise Vs system length for constant Psignal and nonideal filtering

4 channels.,4nm apart(constant Ptotal)
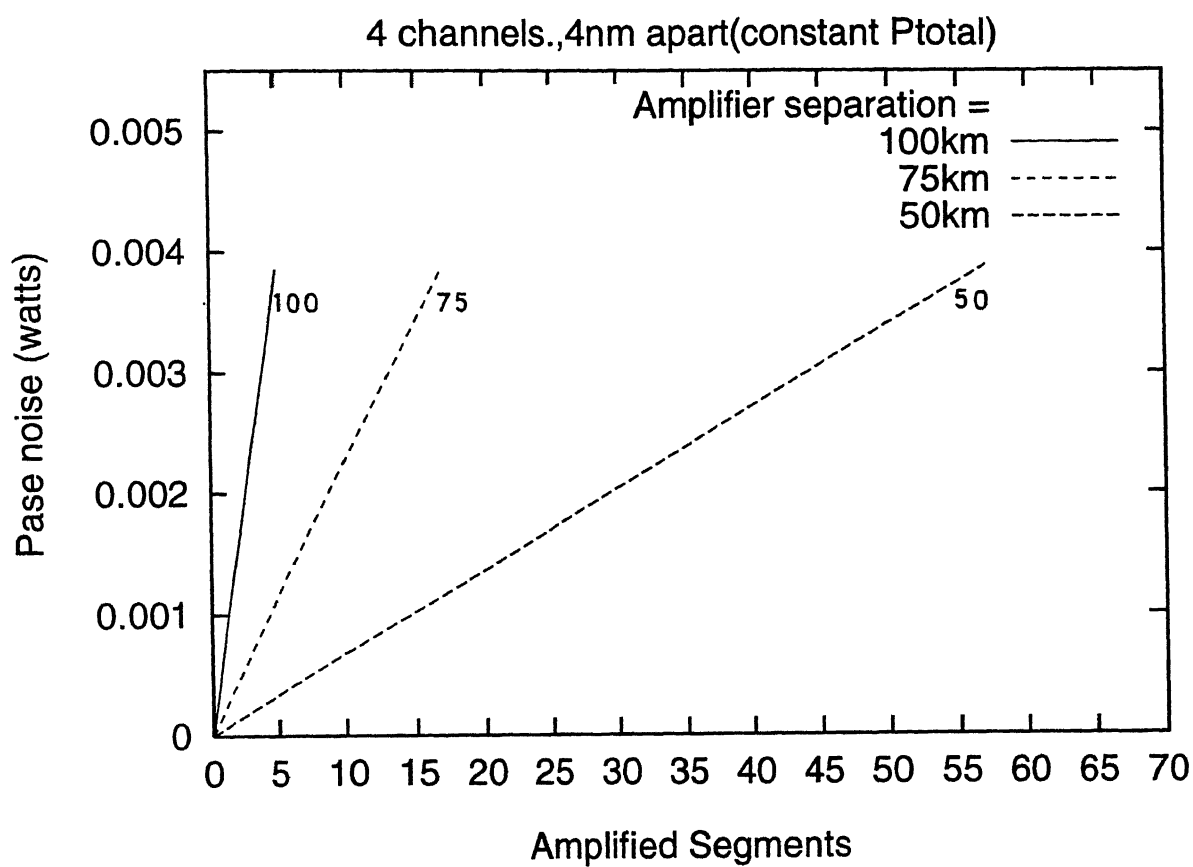
Fig. 3.6 Accumulation of ASE noise Vs system length for different amplifier spacings

CHAPTER - 4
SRS AND FWM LIMITED CASCADED AMPLIFIER SYSTEMS

In the second chapter it was observed that SRS and FWM effects impose a limit on the maximum power transmission per channel to keep the deterioration of the system performance at the minimum. Also in the third chapter, the effect of ASE noise accumulation and the reduction of the end to end bandwidth of the system on the maximum achievable system length, was observed. In this chapter, a combined effect of all the above mentioned factors on the maximum achievable system length, is considered.

4.1 LIMITS IMPOSED BY SRS AND FWM EFFECTS

The limits imposed by the SRS and FWM effects on the maximum achievable system length as shown in Figs. 4.1 to 4.4 are discussed in the following sections.

4.1.1 Constant Total Output Power

Here, the total output power of each amplifier is kept constant and two cases with different channel separation, i.e., 4 nm and 1 nm, are considered.

In Fig. 4.1, it is seen that for a channel separation of 4 nm, the SRS effect is dominant and limits the system length to about 700 km.

Fig. 4.2 shows that for the channel separation of 1 nm, the FWM effect is dominant and limits the system length to just 200 km.

4.1.2 Constant Signal Power

In this case the signal power at the output of each amplifier is kept constant. Figs. 4.3 and 4.4 show the effect of SRS and FWM on the system length, for a channel separation of 4 nm and 1

4 channels separated by 4nm
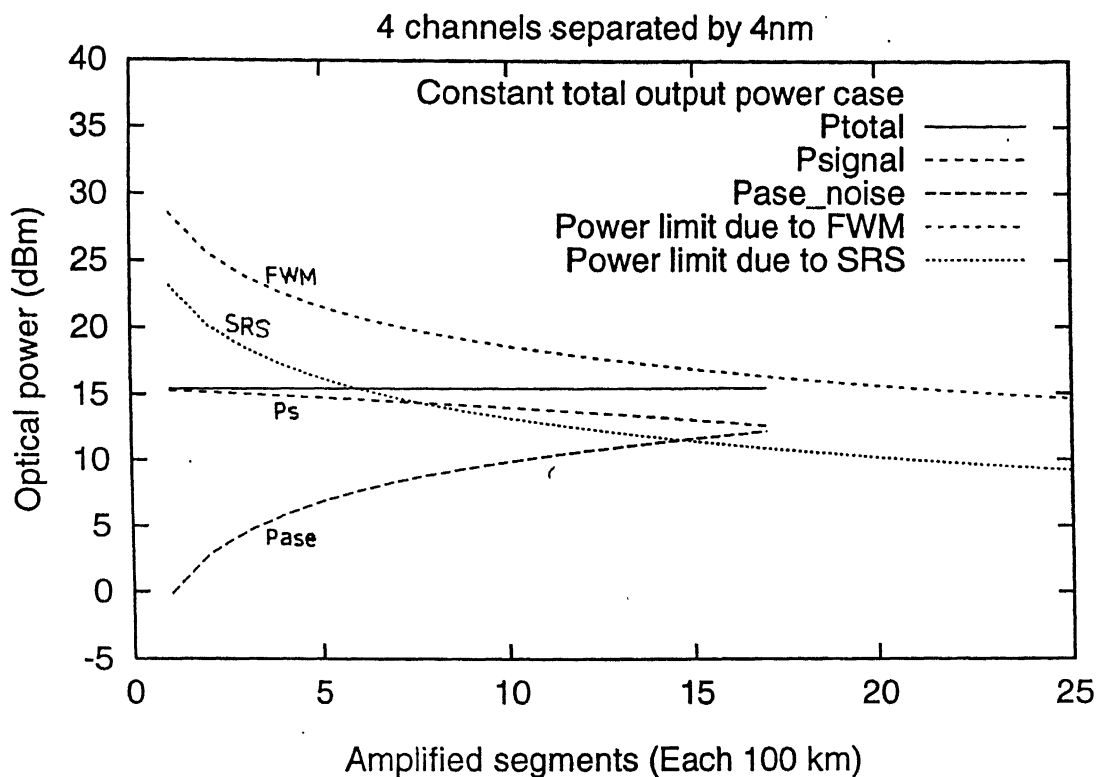
Fig. 4.1 Limits on system length due to FWM and SRS effects for constant Ptotal and $\Delta f = 4nm$.

4 channels separated by 1nm
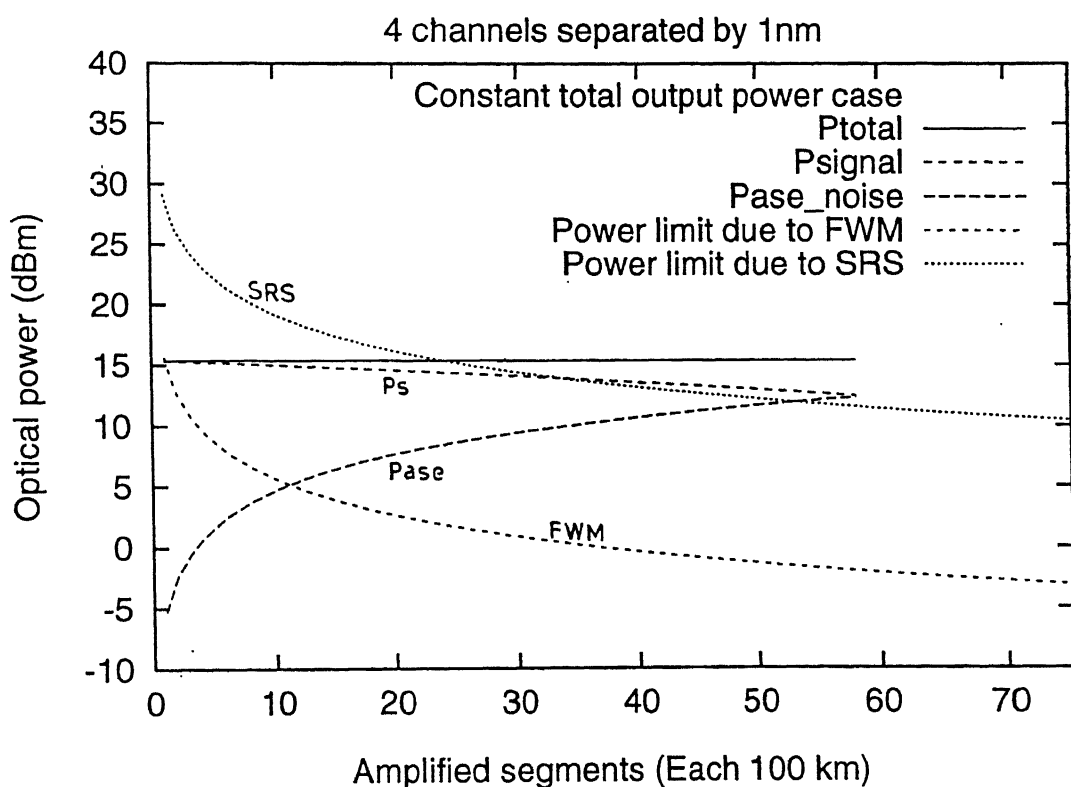
Fig. 4.2 Limits on system length due to FWM and SRS effects for constant Ptotal and $\Delta f = 1nm$

4 channels separated by 4nm
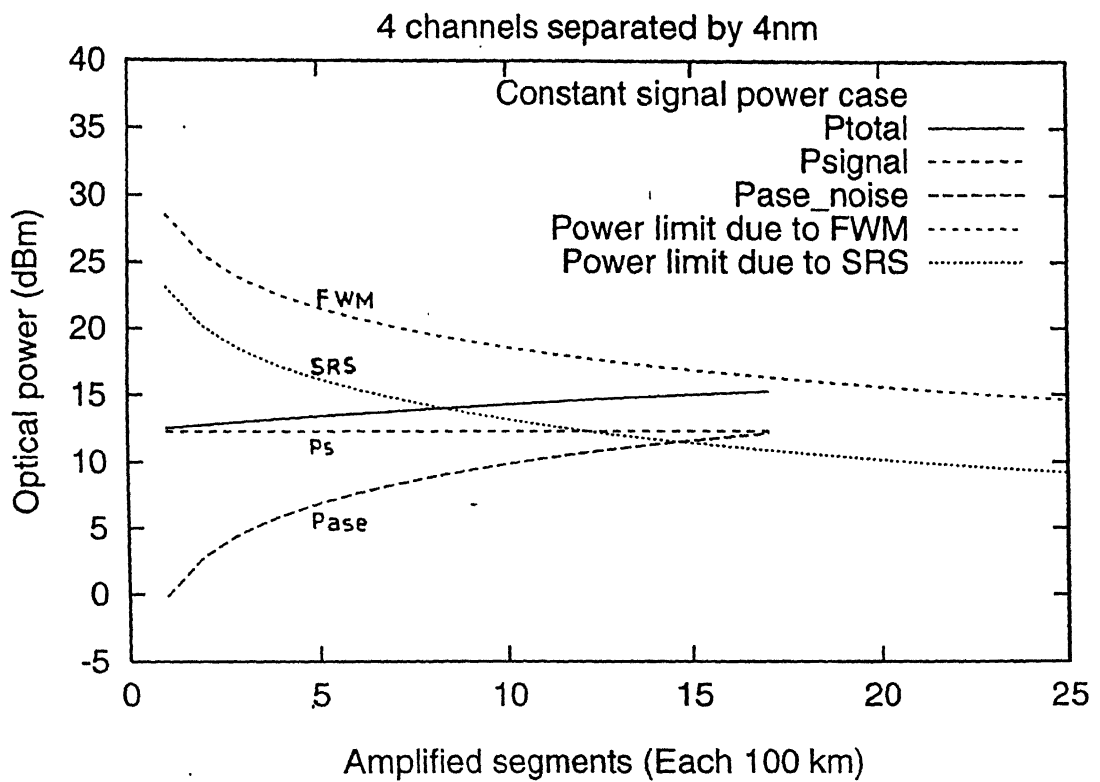
Fig. 4.3 Limits on system length due to FWM and SRS effects for constant Psignal and $\Delta f = 4$nm.

4 channels separated by 1nm
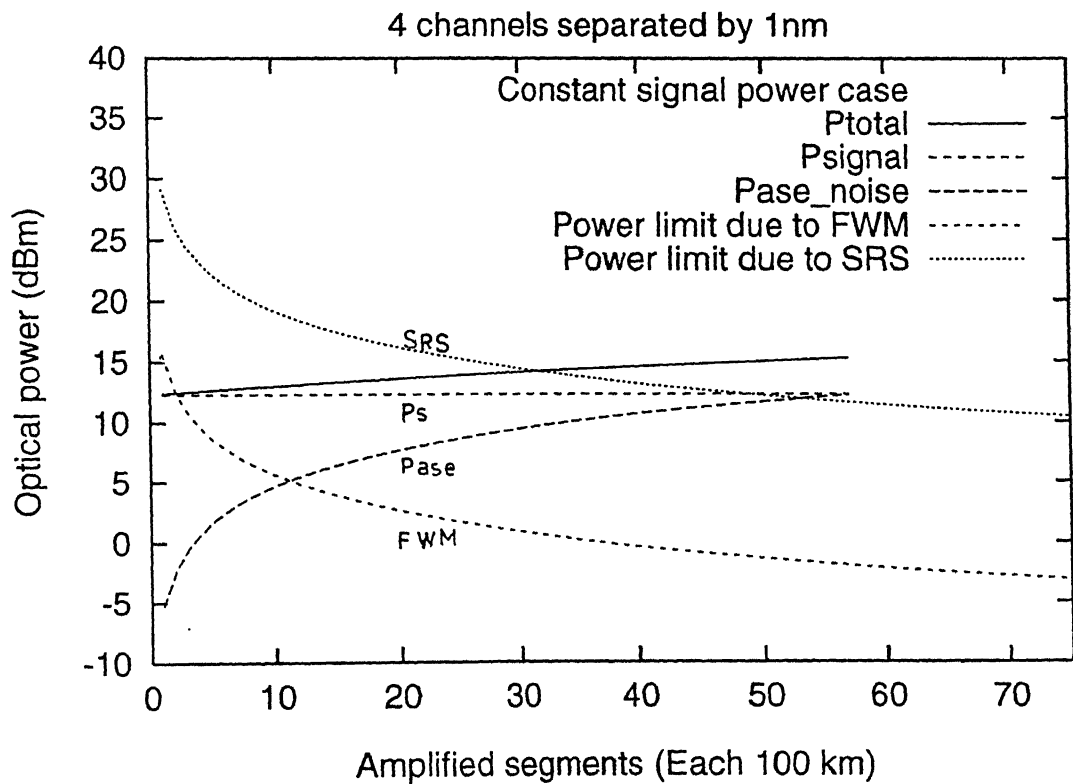
Fig. 4.4 Limits on system length due to FWM and SRS effects for constant Psignal and $\Delta f = 1$nm.

nm, respectively. It is observed that the system length allowed in this case is almost equal to the system length allowed in the case of constant total output power.

So upon comparing the constant total output power and the constant signal power cases, it is observed that the performance in terms of noise is similar in both. So the choice of a particular method may be based upon the issues of system operation and maintenance, rather than noise [7].

For example, the constant total output power monitoring may reduce the hardware complexity as the signal does not have to be independently sensed. For the remaining discussions only the constant total output power case is considered.

4.2 ROLE OF THE COUPLED POWER

It is observed from Figs. 4.1 to 4.4, that with a decrease in the coupled power $P_{s,o}$, the limits due to SRS and FWM effects on the maximum achievable system length relax. So an increase in the system length can be achieved. But, the required P_s/P_{ase} ratio at the receiver puts a limit on the decrease of the $P_{s,o}$.

To study the effect of a decrease of $P_{s,o}$ on the maximum achievable system length, the flow chart shown in Fig. 4.5 has been used.

In Fig. 4.5

M_a is the maximum system length in terms of the number of amplified segments for a given P_s/P_{ase} ratio and $P_{s,o}$. M_a is calculated for the constant total output power case, including the effect of cascaded filters on the end-to-end bandwidth.

M_f is a limit on the system length, in terms of the number of amplified segments, due to the FWM effect for a given P_s/P_{ase}

START

INPUT
NUMBER OF CHANNELS, CHANNEL SEPARATION
DATA RATE PER CHANNEL, AMPLIFIER SEPARATION
Ps/Pase RATIO,   COUPLED POWER Ps,0

USING CONSTANT TOTAL OUTPUT POWER CASCADED
AMPLIFIER MODEL CALCULATE   Ma

CALCULATE   Mf

CALCULATE   Ms

IF
Mf <= Ms

YES

NO

IF
Ma <= Ms

YES

NO

IF
Ma <= Mf

NO

YES

DECREMENT Ps,0

PRINT
Ps,0 and Ma

PRINT
Ps,0 and Ma

STOP
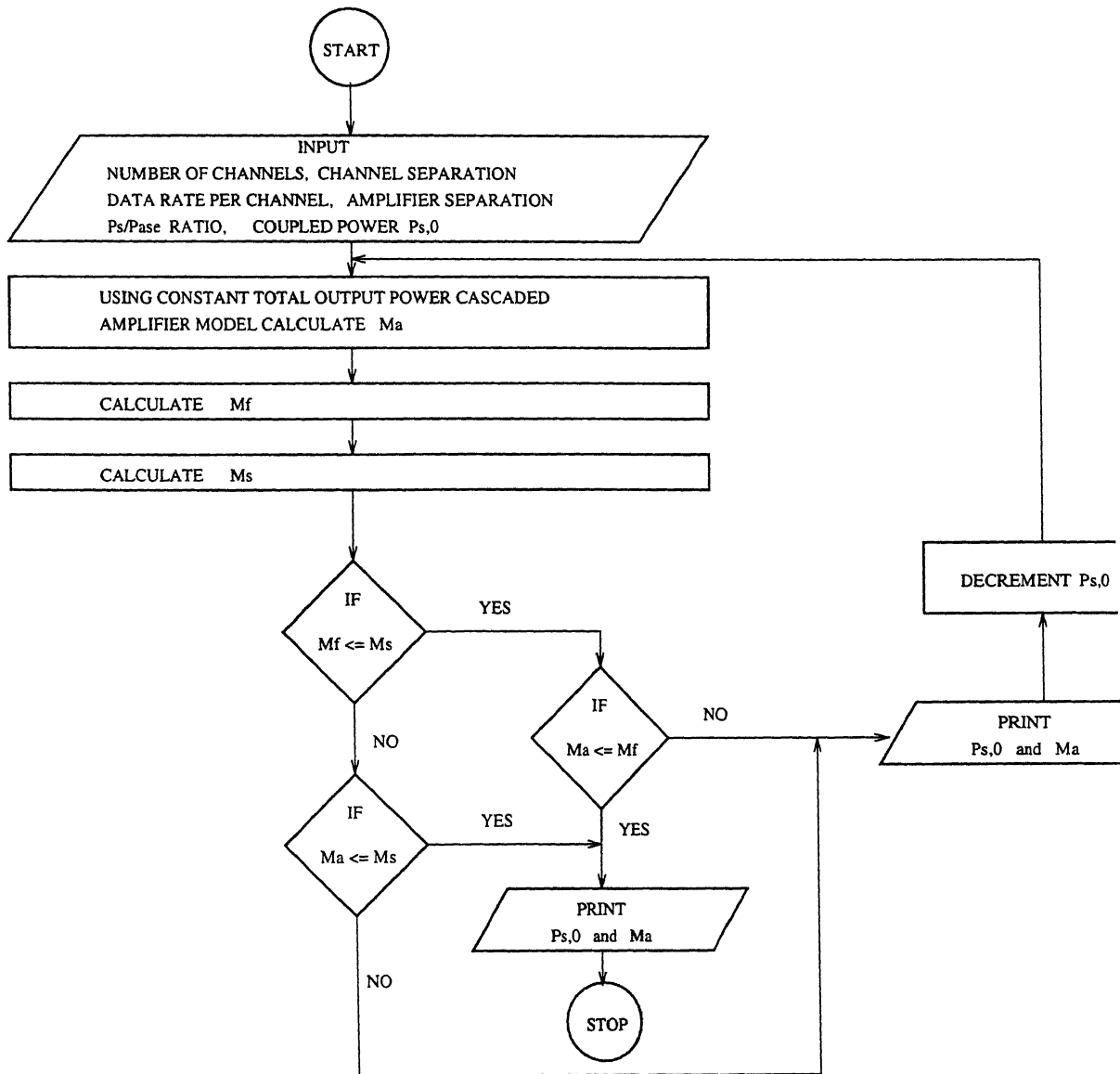
Fig. 4.5 Flow chart for study of the effect of a decrease of Ps,0 on the maximum achievable system len

46

ratio and $P_{s,o}$.

M_s is a limit on the system length, in terms of the number of amplified segments, due to the SRS effect for a given P_s/P_{ase} ratio and $P_{s,o}$.

For a WDM signal consisting of 4 channels with a channel separation of 4 nm, the SRS effect is dominant. As shown in fig. 4.6, $M_s = 7$, $M_a = 13$ and $M_f = 22$ for $P_s/P_{ase} = 2$. As $P_{s,o}$ decreases, M_s and M_f increases but M_a decreases and for $P_{s,o} \simeq$ 22.5 mw,, $M_s = M_a = 10$. So the system length increases from 700 km to 1000 km. With further decrease in $P_{s,o}$ M_a becomes less than M_s, so no additional gain in the system length is achieved.

In another case, a WDM signal, consisting of 4 channels and a channel separation of 1 nm, is considered. As shown in Fig. 4.7, in this case FWM effect is dominant, so $M_f = 2$, $M_a = 40$ and $M_s = 27$. Here again due to a decrease in $P_{s,o}$ to about 5 mW, the system length increases from 200 km to 800 km.

So the coupled power plays a crucial role in keeping the effects due to SRS and FWM at the minimum and deciding the maximum achievable system length.

The above mentioned limit on the maximum achievable system length is not the final one. This limit can be exceeded, depending upon the required bit-error-rate at the receiver, which is discussed in detail in the next chapter.

Data rate/channel= 2.5 Gbits/sec.

4 Channels Separated by=4nm,Ps/Pase=2

Ma ———
Ms - - - -
Mf - - - -

Mf

Ma

Ms

Amplified segments each 100 km long

Power launched in fiber (watts)
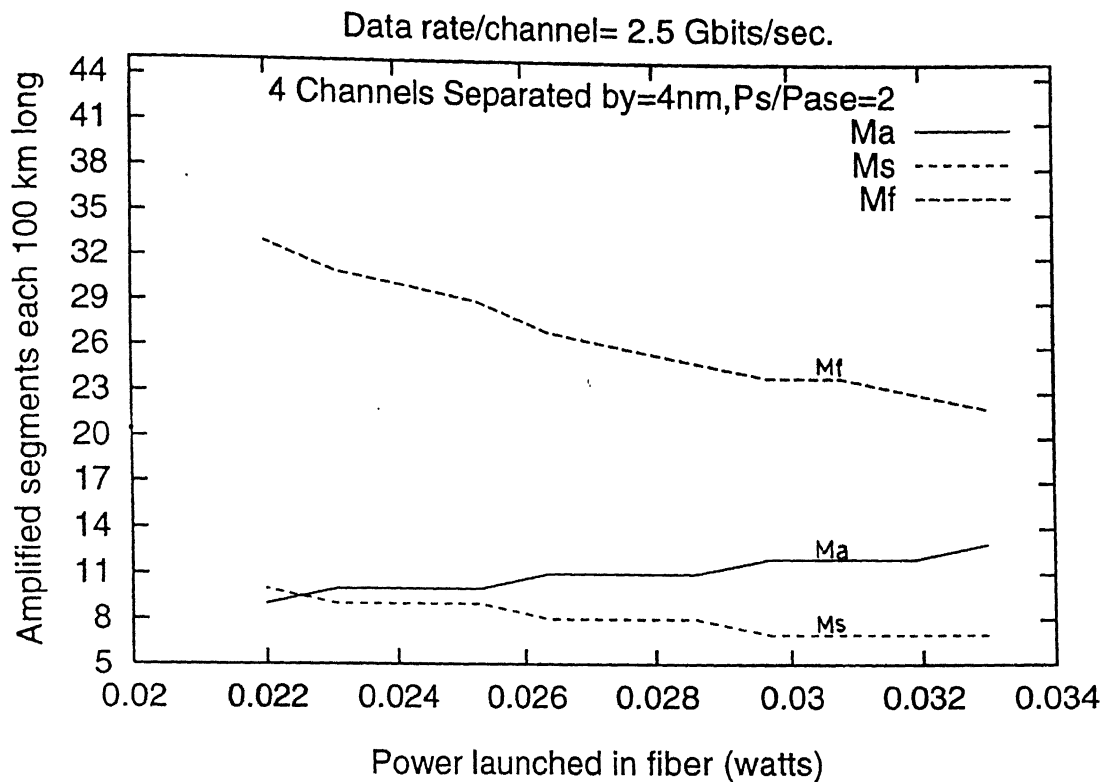
Fig. 4.6 System length Vs coupled power for N = 4 and $\Delta f = 4$nm.

Data rate/channel= 2.5 Gbits/sec.

4 Channels Separated by=1nm,Ps/Pase=2

Ma ———
Ms - - - -
Mf - - - -

Ms

Ma

Mf

Amplified segments each 100 km long

Power launched in fiber (watts)

Fig. 4.7 System length Vs coupled power for N = 4 and $\Delta f = 1$nm.

CHAPTER - 5
THEORETICAL ANALYSIS OF WDM FIBER OPTIC SYSTEM

In this chapter variation of Bit Error Rate (BER) at the output of the receiver, when the limits on the system length imposed by the SRS and FWM effects are exceeded, is considered. Also a variation of the BER with change in the number of channels, channel separation, amplifier spacing and the coupled power is discussed.

5.1 BIT ERROR RATE

In Fig. 5.1 the system block diagram for a N channel WDM fiber optic system with M inline amplifiers has been reproduced. It is assumed that the combiner, splitter and wavelength selective tunable filters do not introduce any cross talk.

Light impinging on the detector (in the receiver) consists of the desired signal, ASE noise and FWM noise. At the receiver, the mean signal currents and noise current variances corresponding to binary '1' and '0' states in the desired wavelength channel (assuming zero signal power during binary '0' states) are expressed as
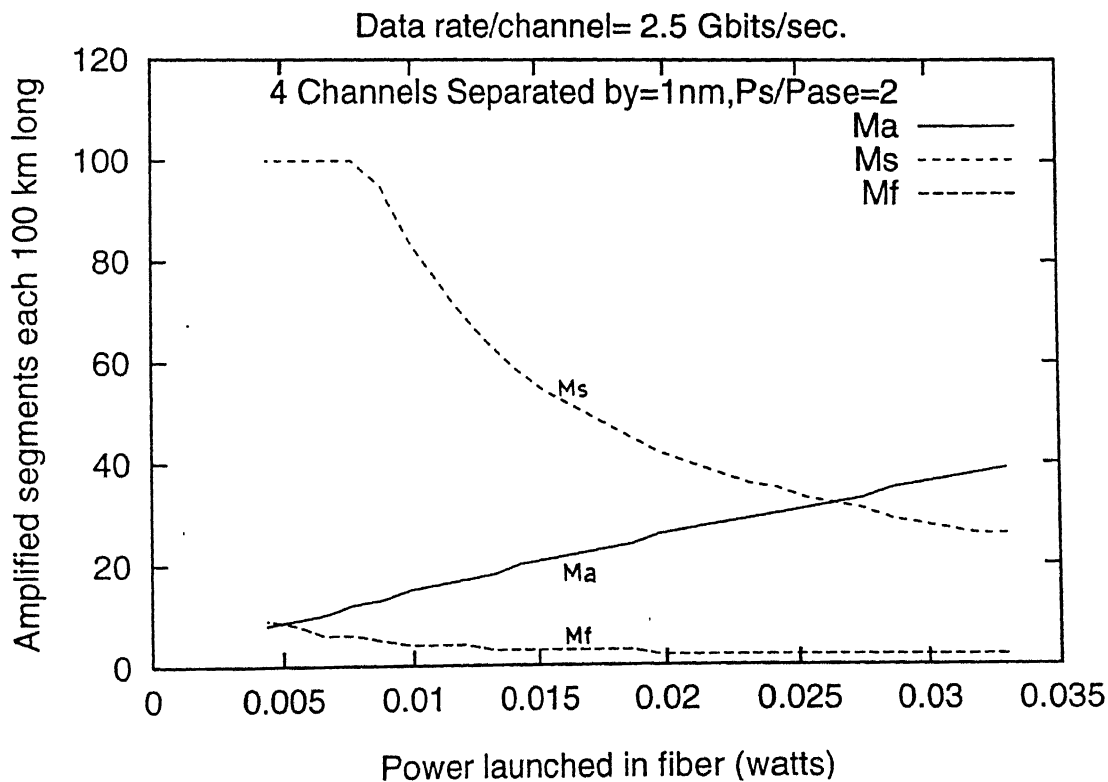
$$I_1 = \frac{e\eta\lambda}{hc} \left(2 \, P_{S,Rx} + P_{ase, \, Rx} + P_{FWM, \, Rx} \right) \qquad (5.1)$$

$$I_0 = \frac{e\eta\lambda}{hc} \left(P_{ase, \, Rx} + P_{FWM, \, Rx} \right) \qquad (5.2)$$

$$\sigma_1^2 = N_{sh}^1 + N_{s-sp} + N_{sp-sp} + N_{s-fwm} + N_{sp-fwm} + N_{th} \qquad (5.3)$$

$$\sigma_0^2 = N_{sh}^0 + N_{sp-sp} + N_{sp-fwm} + N_{th} \qquad (5.4)$$
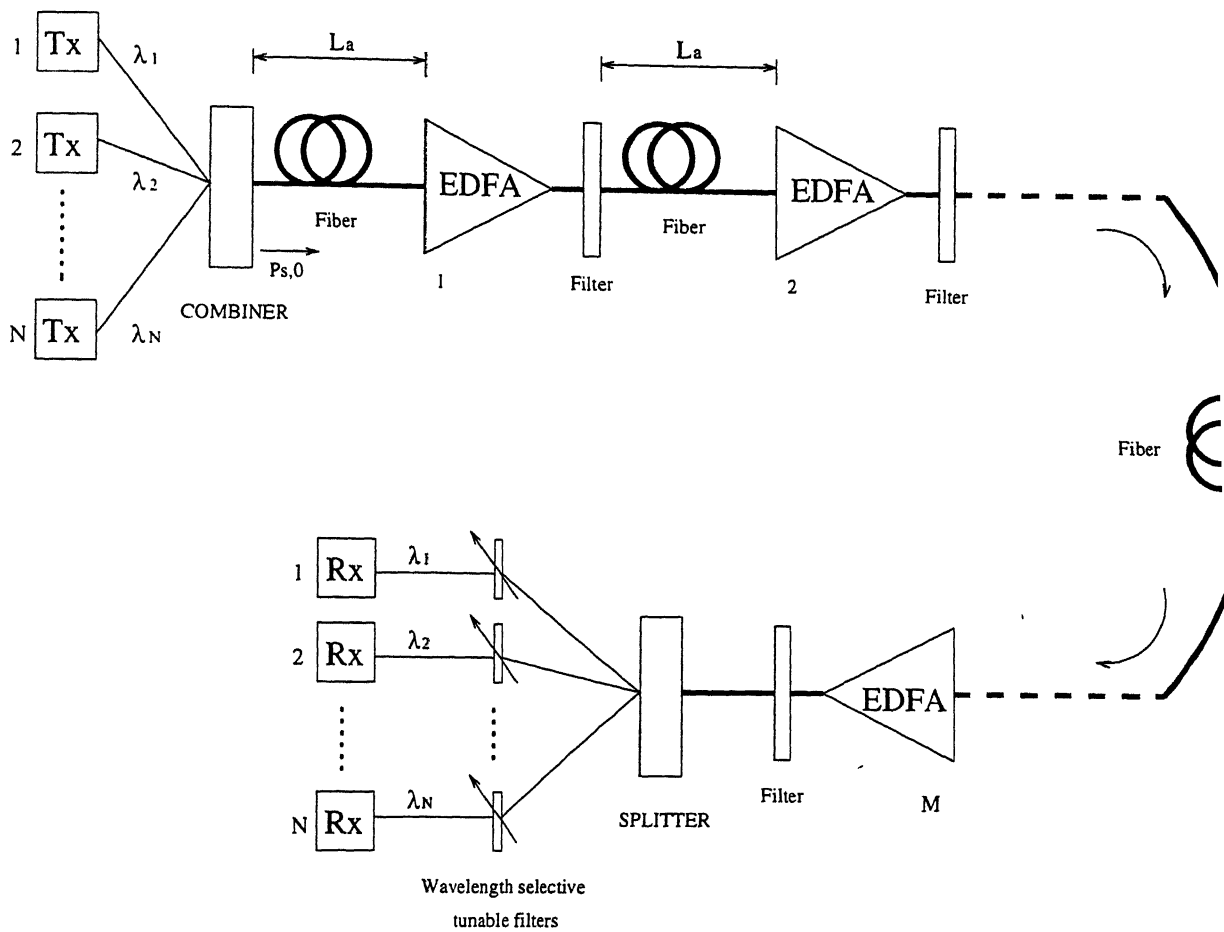
Fig. 5.1 Block schematic of a N channel WDM fiber optic system

where

$$P_{S,Rx} = P_{Signal} \cdot L_T \tag{5.5}$$

$$P_{ase,Rx} = P_{ase} \cdot L_T \tag{5.6}$$

$$P_{FWM,\ Rx} = P_{FWM}(\lambda) \cdot L_T^1 \tag{5.7}$$

L_T = Splitting loss + Tunable filter loss + Connector Loss

L_T^1 = Tunable filter loss + Connector Loss

$P_{FWM}(\lambda)$ is FWM noise power generated at the wavelength λ

η is the quantum efficiency of the detector

h is Plank's constant (6.63×10^{-34} J.s.)

I_1 is the signal current corresponding to binary state '1'

I_0 is the signal current corresponding to binary state '0'

σ_1^2 is the noise current variance corresponding to state '1'

σ_0^2 is the noise current variance corresponding to state '0'

N_{s-sp}, N_{sp-sp}, N_{s-fwm}, N_{sp-fwm}, N_{sh}, N_{th} are signal-ASE, ASE-ASE, Signal-FWM, ASE-FWM beat noise powers, shot noise power and thermal noise power respectively [10,11].

The values of N_{th} and N_{sh} are negligible compared to the other beat noise powers, so can be neglected without any significant change in the BER.

BER for the channel wavelength λ is, [12]

$$BER = 0.5\ \text{erfc}\ \left[\frac{I_1 - I_0}{\sqrt{2}(\sigma_1 + \sigma_0)} \right] \tag{5.8}$$

Also, while calculating BER, the effect of SRS is considered interms of the depletion of the signal power as discussed in the second chapter. The parameter values used for the BER calculations are as follows:

η = 1

A_e (Effective core area of the fiber) = $5 \times 10^{-11} m^2$

D (Fiber chromatic dispersion coefficient) = 2 ps/nm-km

51

$$dD/d\lambda \qquad\qquad = 0.09 \text{ ps/nm}^2\text{-km}$$

α (Fiber loss Coefficient) $\qquad = \qquad 0.25$ dB/km

Data rate per channel $\qquad\qquad = \qquad 2.5$ Gbits/sec

Bandwidth of wavelength selective tunable filter = 125 GHz

Electrical bandwidth of the receiver = 1.25 GHz

Tunable filter loss $\qquad\qquad = \qquad 3$ dB

Total connector loss of the terminal node = 2 dB

The flow chart used for the BER calculation is given in Fig. 5.2.

Here the decrement in the coupled power $P_{S,0}$ is adjusted in such a way that for the decremented value of $P_{S,0}$, the system length for the given P_S/P_{ase} ratio decreases exactly by one segment.

For the constant total output power case

$$P_{S,0} = P_{T,i} \qquad \text{where } i = 1, 2, \ldots\ldots, M \qquad\qquad (5.9)$$

Also from Fig. 3.1

$$P_{T,M} = P_{S,M} + M\, P_{ase} \quad \text{for } i = 1, 2, \ldots\ldots, M \qquad\qquad (5.10)$$

Using equations (5.9) and (5.10),

$$\text{Decrement in } P_{S,0} = (R+1)P_{ase} \qquad\qquad (5.11)$$

where R is the given P_S/P_{ase} ratio.

Note that P_S/P_{ase} is the ratio of the signal power to the cumulative ASE noise power and P_{ase} in equation (5.11) is the ASE noise contributed by one amplifier.

5.1.1 Variation of Bit Error Rate with System Length

The variation of BER with system length, for the given P_S/P_{ase} ratio and amplifier spacings of 100 km, 75 km and 50 km, is shown in Figs. 5.3, 5.4 and 5.5. It is observed that for $P_S/P_{ase} = 1.75$ and BER $= 10^{-10}$, the maximum achievable system
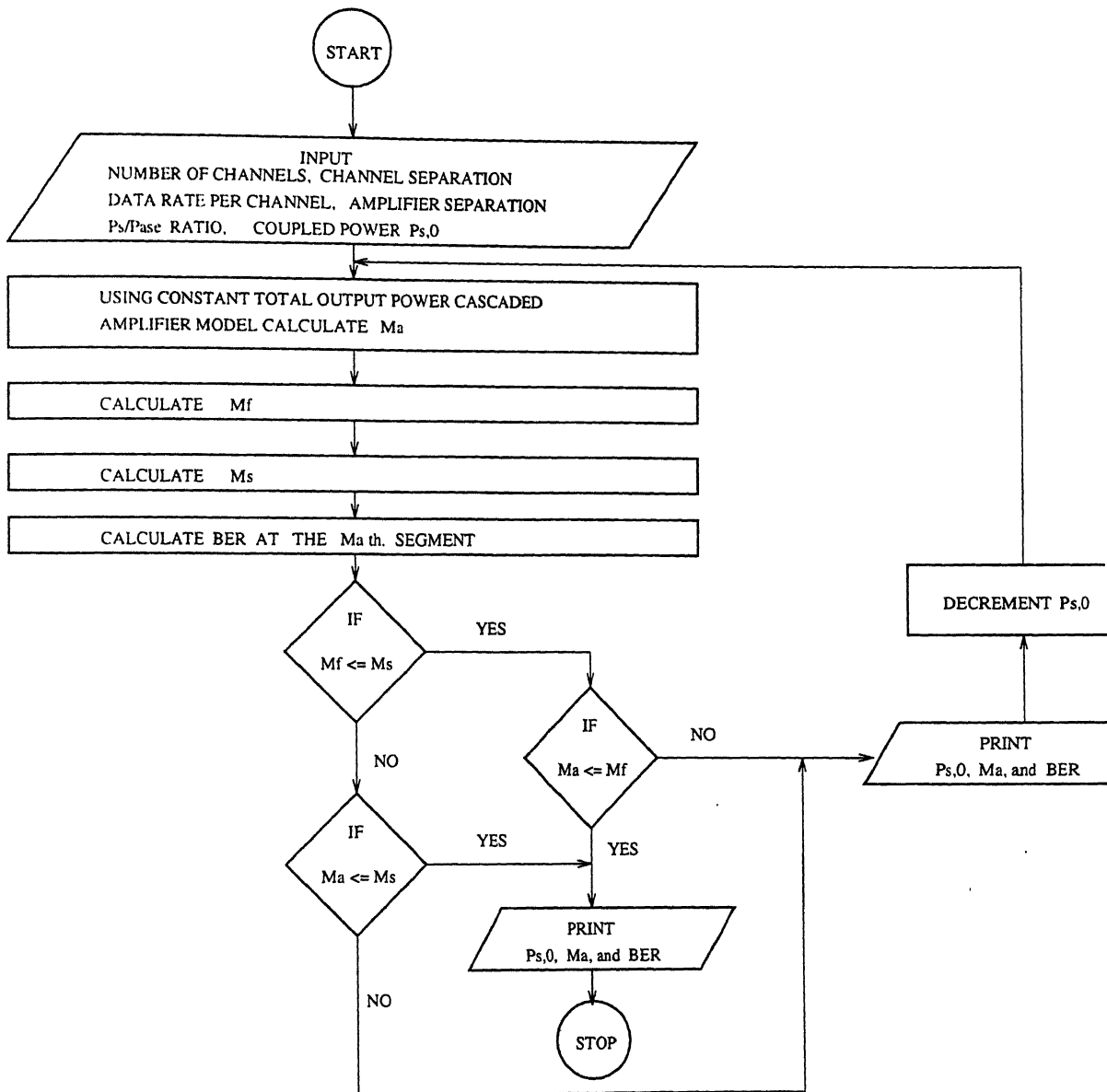
Fig. 5.2 Flow chart for study of variation of the BER with the system length

length is 1200 km, 1950 km and 2600 km for the amplifier separation of 100 km, 75 km and 50 km, respectively. Also it is observed that for all the three cases, i.e., for amplifier separation of 100 km, 75 km and 50 km, with increase in P_S/P_{ase} ratio the variation in BER increases with system length. This is because of the fact that for small P_S/P_{ase} ratio, the ASE noise is dominant and suppresses the effects of SRS and FWM, but with increase in the P_S/P_{ase} ratio the relative dominance of the ASE noise decreases. So the FWM and SRS effects degrade the system performance, with the increase in the system length, at a faster rate.

5.1.2 Effect of Number of Channels on BER

Figs. 5.6, 5.7 and 5.8 give variation of the BER with change in the number of channels for a given channel separation, system length and P_S/P_{ase} ratio. Again three cases with different amplifier separation, i.e., 100 km, 75 km and 50 km, are considered. In the figures it is seen that BER increases with an increase in the number of channels for a given system length and P_S/P_{ase} ratio. The reason for this is that with an increase in the number of channels, the SRS and FWM effects increases and also the bandwidth of the WDM signal increases which in turn increases the ASE noise generated by the amplifiers.

It is seen from Figs. 5.3 to 5.5 that for a WDM signal consisting of 4 channels with 4 nm channel separation, each having a data rate of 2.5 Gbits per second and for P_S/P_{ase} = 1.75, the maximum achievable system length for BER = 10^{-10} is 1200 km, 1950 km and 2600 km for the amplifier spacing of 100 km, 75 km and 50 km, respectively. So the 50 km amplifier separation is the best

Data Rate/Channel = 2.5 Gbits/sec.

4 Channels separated by 4nm., Ps/Pase =

1.5	————
1.75	- - - - -
2.0	— — —
2.5	········
3.5	·········
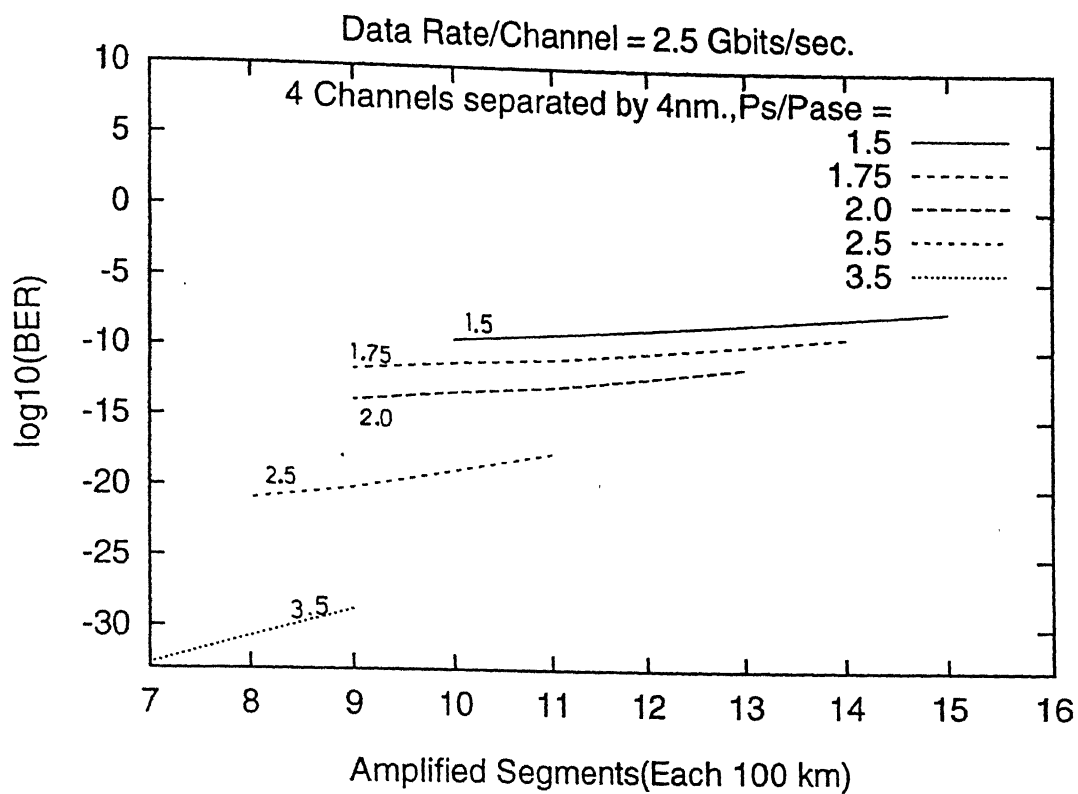
Fig. 5.3 BER Vs system length for different values of Ps/Pase ratio. (La = 100 km.)

Data Rate/Channel = 2.5 Gbits/sec.

4 Channels separated by 4nm., Ps/Pase =

1.5	————
1.75	- - - - -
2.5	— — —
3.5	········
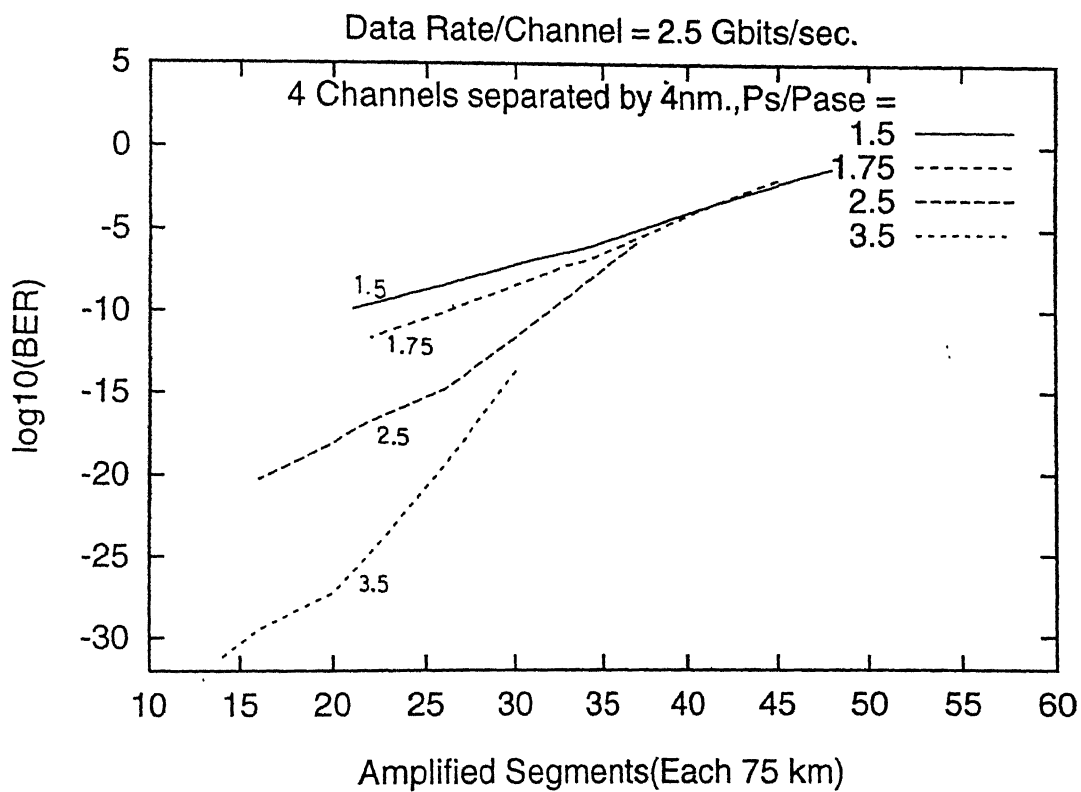
Fig. 5.4 BER Vs system length for different values of Ps/Pase ratio. (La = 75 km.)

Data Rate/Channel = 2.5 Gbits/sec.

4 Channels separated by 4nm.,Ps/Pase =
1.5 ———
1.75 --------
2.5 -------
3.5 ·········

Fig. 5.5 BER Vs system length for different values of Ps/Pase ratio. (La = 50 km.)

Data Rate/Chanel = 2.5 Gbits/sec.

Channel separation = 1nm.,Ps/Pase=3.5, N=
8 ———
12 --------
16 -------

Fig. 5.6 BER Vs system length for different number of channels. (La = 100 km.)

56

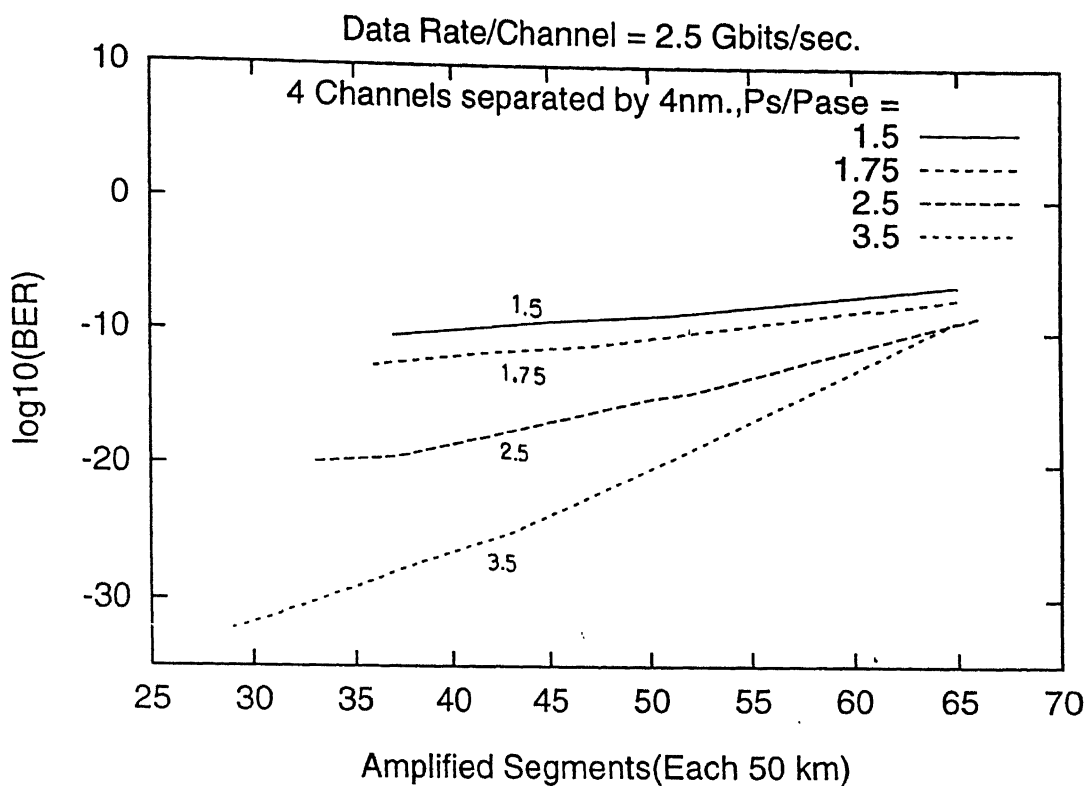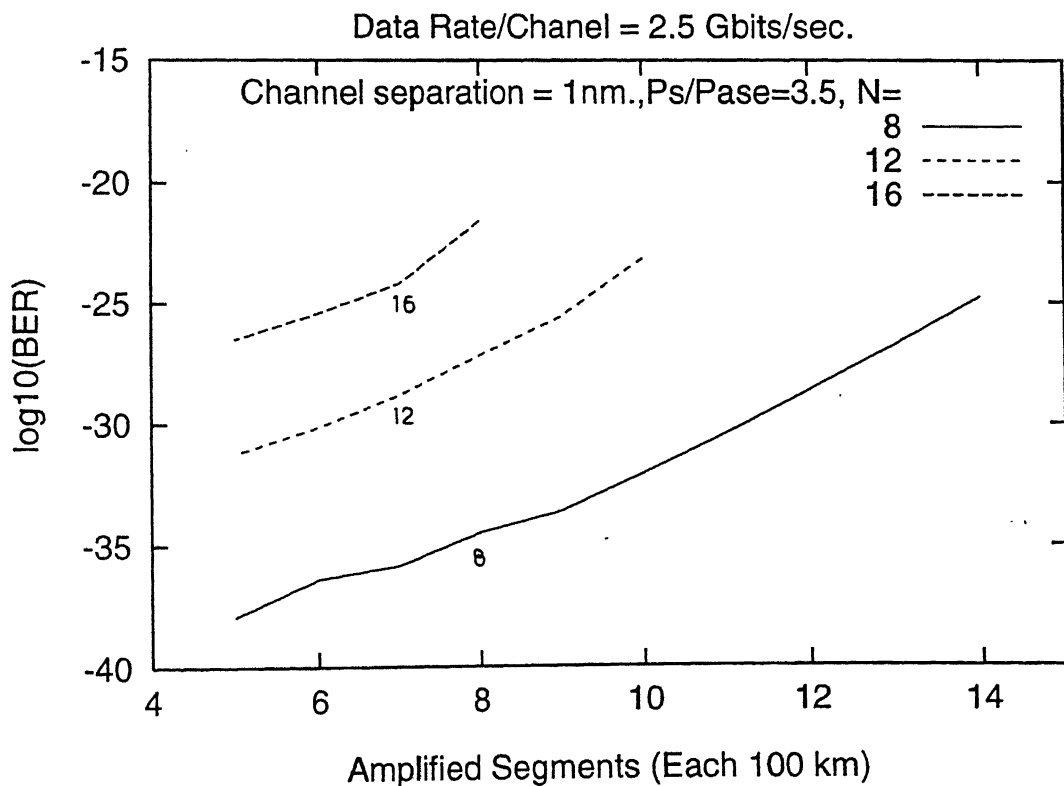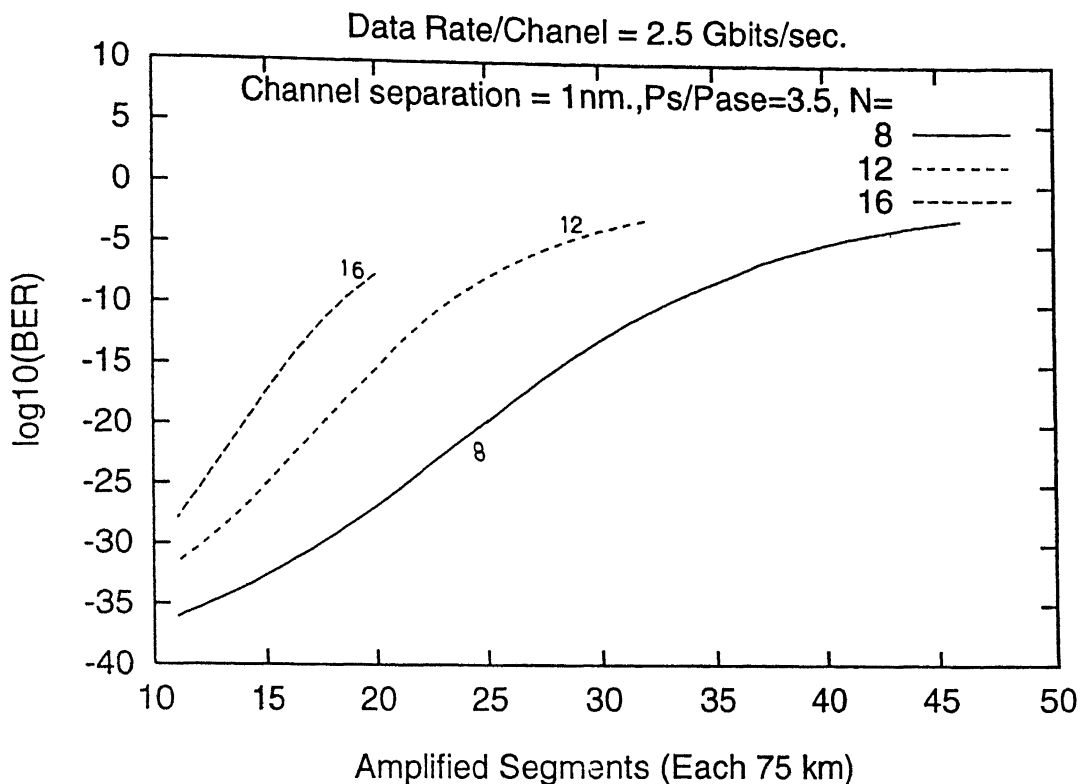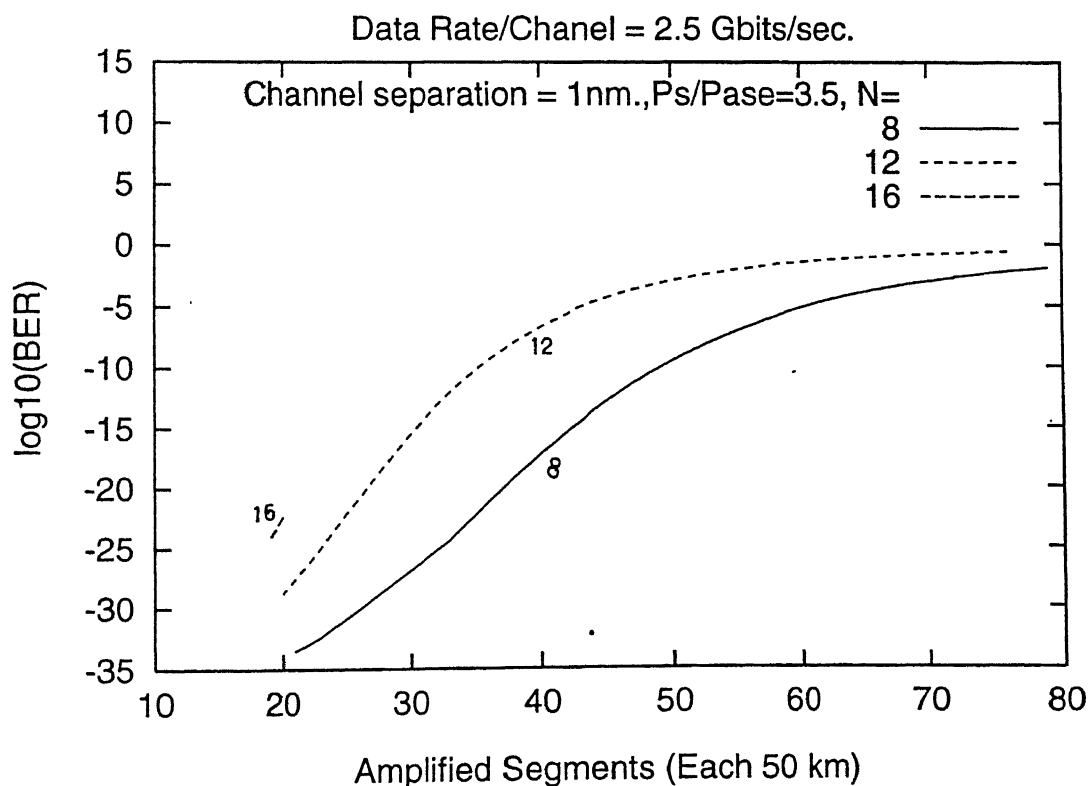Fig. 5.7 BER Vs system length for different number of channels. (La = 75 km.)

Fig. 5.8 BER Vs system length for different number of channels. (La = 50 km.)

in this case as it gives the maximum system length.

In Figs. 5.7 and 5.8, for the WDM signal consisting of 12 channels separated by 1 nm, for BER $= 10^{-10}$, the system length achieved is about 1700 km for both the 50 km and 75 km amplifier separations. So the choice of amplifier separation is dependent on both the number of channels and the channel separation.

5.1.3 Variation of BER with P_S/P_{ase} Ratio

In Figs. 5.9, 5.10 and 5.11, variation of BER with increase in P_S/P_{ase} ratio in the 11th segment, for the given segment length (amplifier separation), number of channels and channel separation, is considered.

In the figures it is seen that with the increase in P_S/P_{ase} ratio the BER, for 100 km, 75 km and 50 km amplifier separation, tends to reach a floor. This occurs earlier, i.e., for smaller P_S/P_{ase} values, as the segment length increases. This effect is more pronounced in Fig. 5.11. The reason for this effect is that with the increase in P_S/P_{ase} ratio, ASE noise remains the same, but, the effect of FWM and SRS increases because of the increase in the signal power, and at a certain point the increase in the SRS and FWM effects matches the increase in the signal power. Also it is observed in Fig. 5.11 that, for the case of 75 km amplifier separation, saturation in the BER value occurs at $P_S/P_{ase} \simeq 5$.

In the next chapter, degradation of the system performance due to crosstalk in the space switches at the terminal node will be considered.

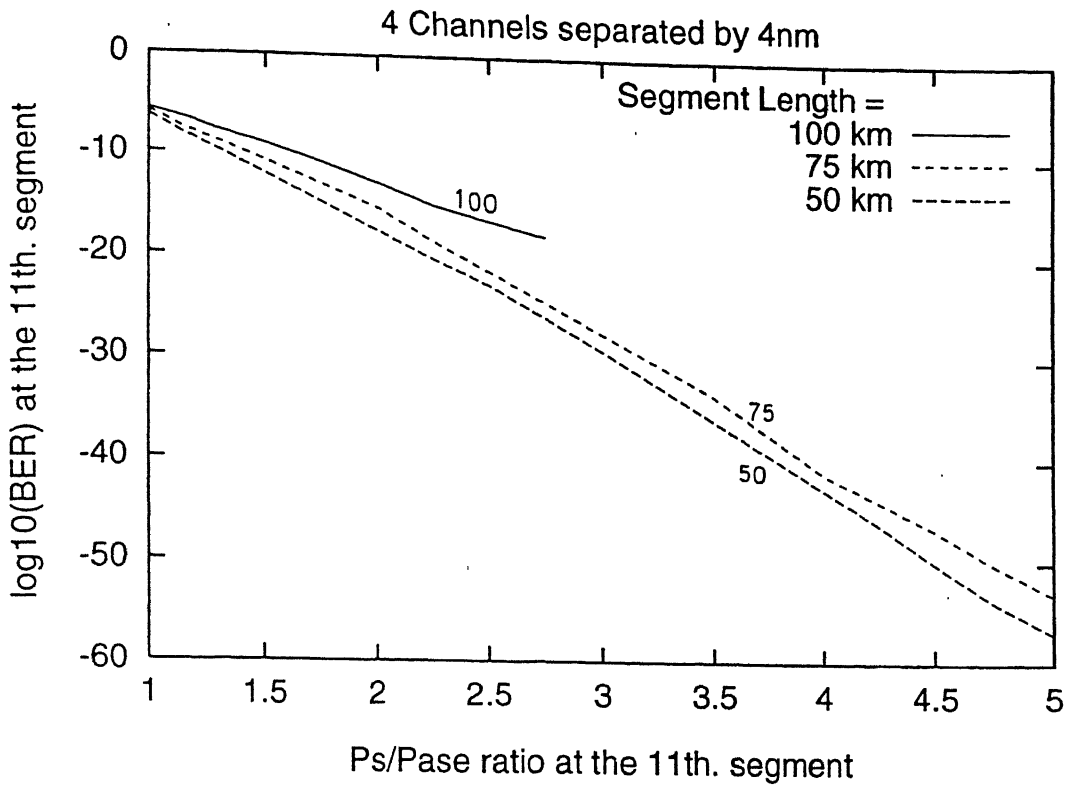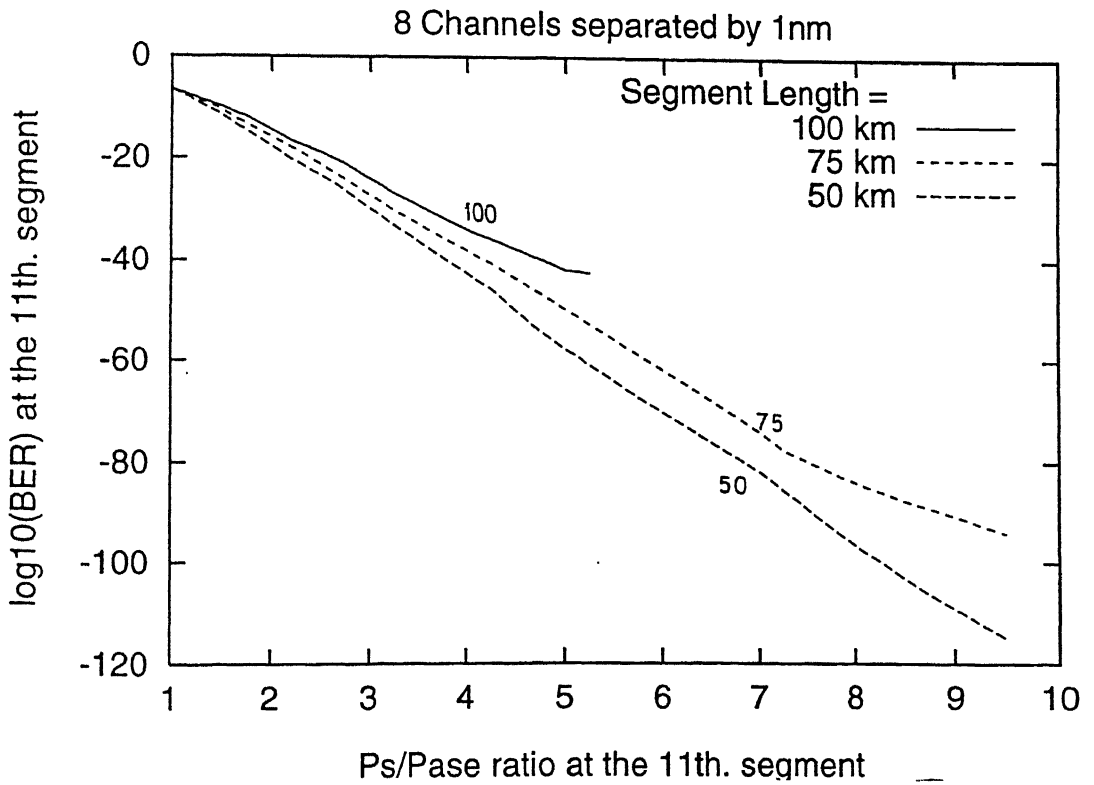Fig. 5.9   BER Vs Ps/Pase ratio for Ma = 11, N = 4, $\Delta f = 4nm$.

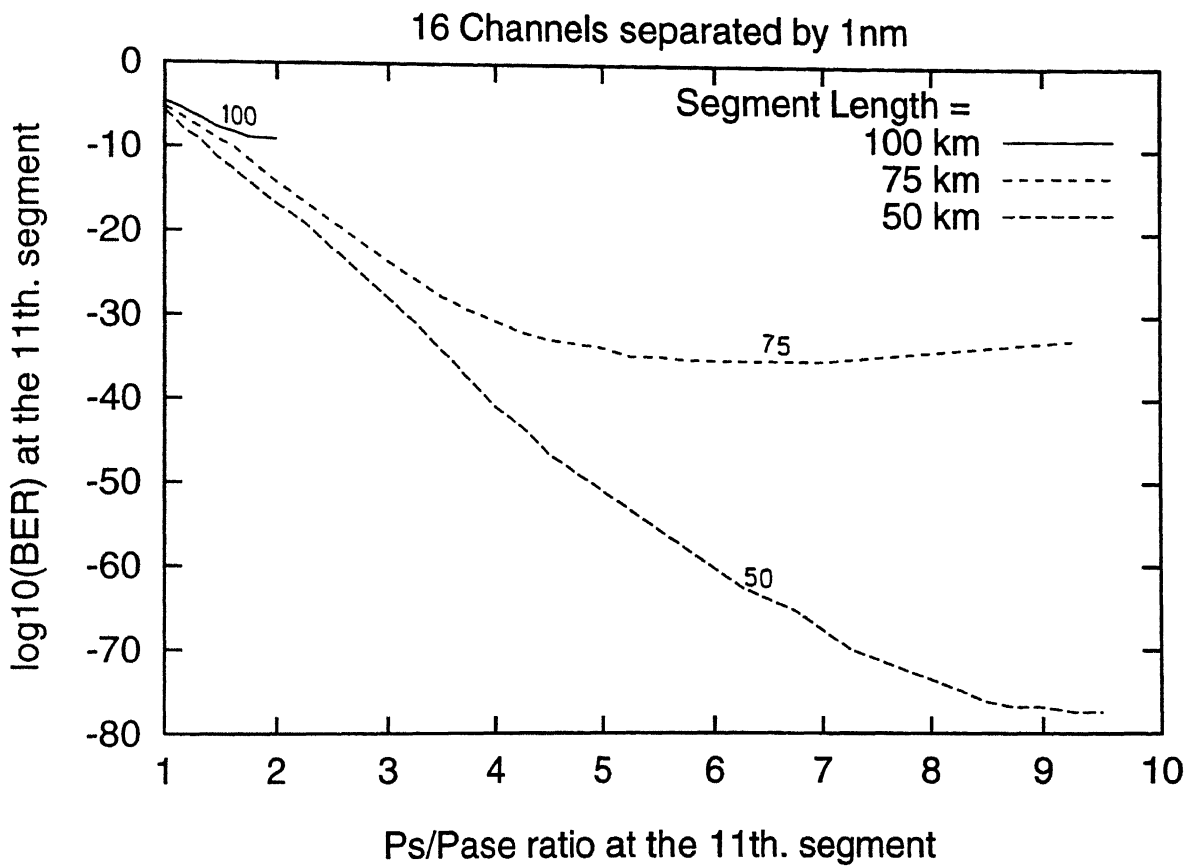Fig 5.10   BER Vs Ps/Pase ratio for Ma = 11, N = 8, $\Delta f = 1nm$.

Fig. 5.11   BER   Vs   Ps/Pase ratio for Ma = 11, N = 16, $\Delta f = 1nm$.

CHAPTER - 6
OPTICAL SPACE SWITCHING

At the terminal node where more than one fibers are terminating and according to the requirement of the network, some selected channels from each input fibers are to be routed to one outgoing fiber without optical to electrical and back to optical conversion. In such a situation for dynamic wavelength routing, optical space switches are used. But these switches cause degradation of the system performance due to introduction of switch cross talk. It is discussed in detail in the following sections.

6.1 CHOICE OF SWITCH ARCHITECTURE

The basic switch element of a 1x1 optical space switch is a 2x2 optical switch. Switch elements can be directional coupler switches or Mach Zehnder Interferometer (MZI) switches fabricated on titanium diffused lithium niobate (Ti:LiNbO$_3$) substrates. Because of the electro-optic properties of LiNbO$_3$ the switch elements can be made to operate in bar state or cross state (Fig. 6.1) by the application of a suitable voltage. Note that a 2x2 optical space switch has only one cross point whereas a 2x2 electrical switch has four cross points. In the cross state some power leakage from input 1 to output 3 due to some manufacturing defects leads to crosstalk among the signals at outputs 3 and 4. More is the number of such cross points in an optical path, more is the cross talk. Many such switch elements are interconnected in different manners to make a 1x1 switch. Several optical switch architectures are suggested [14], such as,
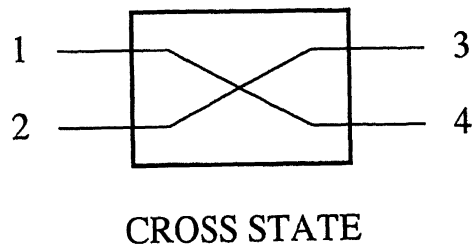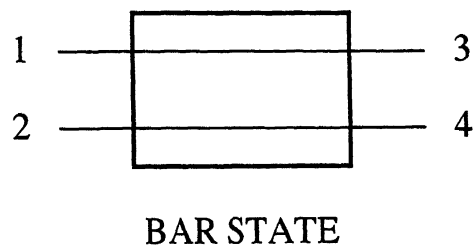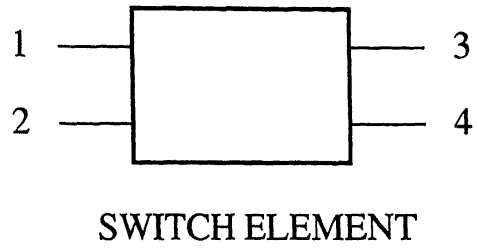
Fig. 6.1   Basic switch element in Bar and Cross states

- Crossbar architecture
- N-stage planar architecture
- Double crossbar architecture
- Benes architecture

The total number of switch elements and the number of stages of switch elements, i.e., the number of columns in the switch matrix vary for the different architectures as given below for 1x1 switch.

ARCHITECTURE	NUMBER OF SWITCH ELEMENTS	NUMBER OF COLUMNS
Cross bar	1^2	1
N-stage planar	$1(1-1)/2$	1
Double crossbar	21^2	$1+1$
Benes	$(1/2)(2\log_2 1 - 1)$	$2\log_2 1 - 1$

Among the four architectures mentioned above, the Benes architecture has the least number of stages of switch elements. So in the discussion of BER degradation, Benes architecture is considered. A 8x8 optical space switch using Benes architecture is shown in Fig. 6.2.

6.2 BER DEGRADATION DUE TO SPACE SWITCH CROSS TALK

For the requirement of dynamic wavelength routing at the terminal node, the optical space switches are incorporated as shown in Fig. 1.4 and 1.5. The space switches in the optical path degrade the BER depending upon the crosstalk level per cross point. Assuming equal crosstalk in every cross point, the maximum optical switch crosstalk at the receiver is given as

$$I_{X\ max} = R.I_X \qquad (6.1)$$

where R is the number of the space switch cross points in the optical path, and I_X is the crosstalk contribution per cross
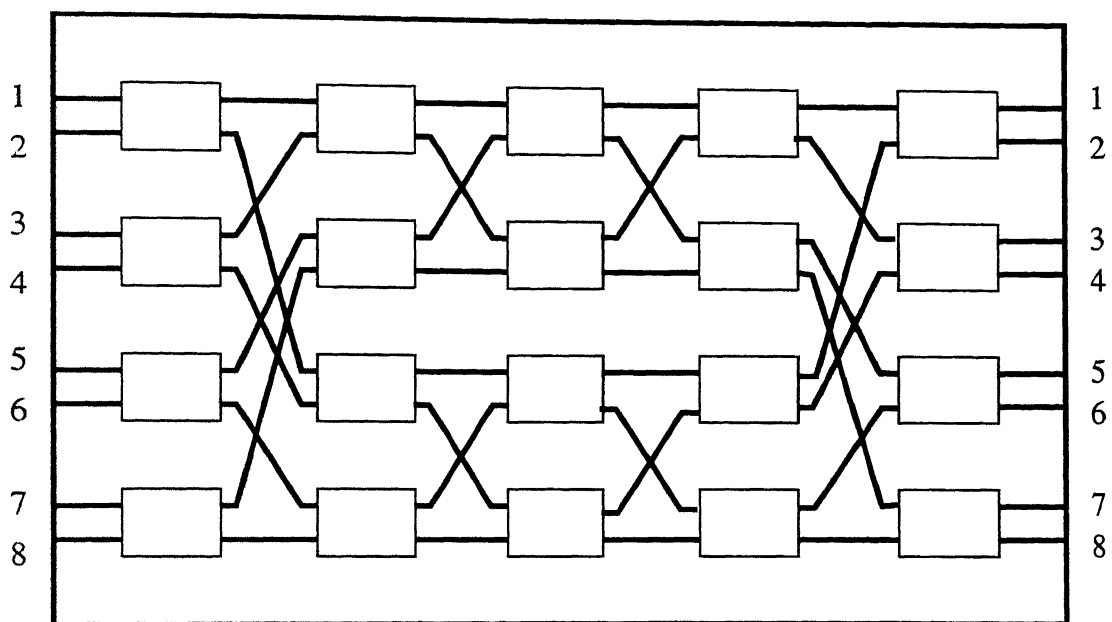
Fig. 6.2   8x8 optical space switch using Benes architecture

point.

In an ON-OFF keyed system, assuming no crosstalk contribution due to '0' state of the signal, the number of '1' state crosstalk signals is binomially distributed and takes R+1 possible values with the probability [13],

$$P_B \ (r = i) = \frac{R!}{i! \ (R-i)!} \left(\frac{1}{2}\right)^R \tag{6.2}$$

where i = 0, 1, 2,...., R

Taking the switch crosstalk into account, the equation (5.8) is modified as [12, 13],

$$BER = 0.25 \sum_{i=0}^{R} \left\{ erfc\left[\frac{|D - (I_1 + rI_X)|}{\sqrt{2} \ \sigma_1}\right] + erfc\left[\frac{|D - (I_0 + rI_X)|}{\sqrt{2} \ \sigma_0}\right] \right\}$$

$$\cdot P_B(r=i)$$

$$\tag{6.3}$$

Where D is the optimum threshold chosen numerically to obtain the minimum BER in each case.

For the determination of optimum D numerically, it is made to cover the range $(I_D - I_D/2)$ to $(I_D + I_D/2)$ in 80 steps.

where $I_D = \left[\frac{(I_1 + rI_X) + (I_0 + rI_X')}{2}\right]$

For each step, BER is calculated and the value of D corresponding to the minimum BER is chosen as the optimum threshold. The same procedure is repeated for different values of r.

The number of columns in a (1x1) optical space switch, using Benes architecture, is $(2 \log_2 l) - 1$. So for one 1x1 optical space switch in the optical path, the maximum number of cross points is R = $(2 \log_2 l) - 1$, where 1 depends upon the number of the optical

fibers entering the node.

The degradation of the BER due to an increase in the crosstalk per cross point is given in Figs. 6.3 and 6.4. Also the degradation of the BER due to an increase in the number of cross points in the optical path for a given crosstalk per cross point is shown in Figs. 6.5 and 6.6.

In Fig. 6.3 for P_s/P_{ase} = 1.75 and the system length of 1200 km, BER is 10^{-10} with switches having zero crosstalk (-∞ dB). For -25 dB crosstalk per cross point, there is marginal increase in the BER. For -15 dB crosstalk per cross point BER increases to 10^{-9}, and for -10dB crosstalk, BER becomes more than 10^{-8}. Similar results are shown in Fig. 6.4 for a different amplifier spacing, i.e., 75 km and the WDM signal consisting of 8 channels with 1 nm channel separation.

In Fig. 6.5, crosstalk per cross point is kept constant of -10 dB. With 4 input fibers at the terminal node, at about 1275 km, the BER $\approx 10^{-10}$ and it increases to about 10^{-7} with the increase in the number of input fibers to 64. It is because of the fact that the number of cross points in the optical path increases with the increase in the number of the input fibers.

It has been observed from Figs. 6.3 and 6.4 that the space switches with crosstalk per cross point equal to -25 dB degrade the system performance almost negligibly. So for large networks with a large number of space switches in an optical path, switches with crosstalk level per cross point less than -25 dB are required to avoid a degradation in the system performance.

8 I/P fibers/node, 4 Channels separated by 4nm./fiber

Ps/Pase = 1.75, Crosstalk/crosspoint =
-10 dB ———
-15 dB - - - - -
-25 dB — — —
- Infinity dB ·········
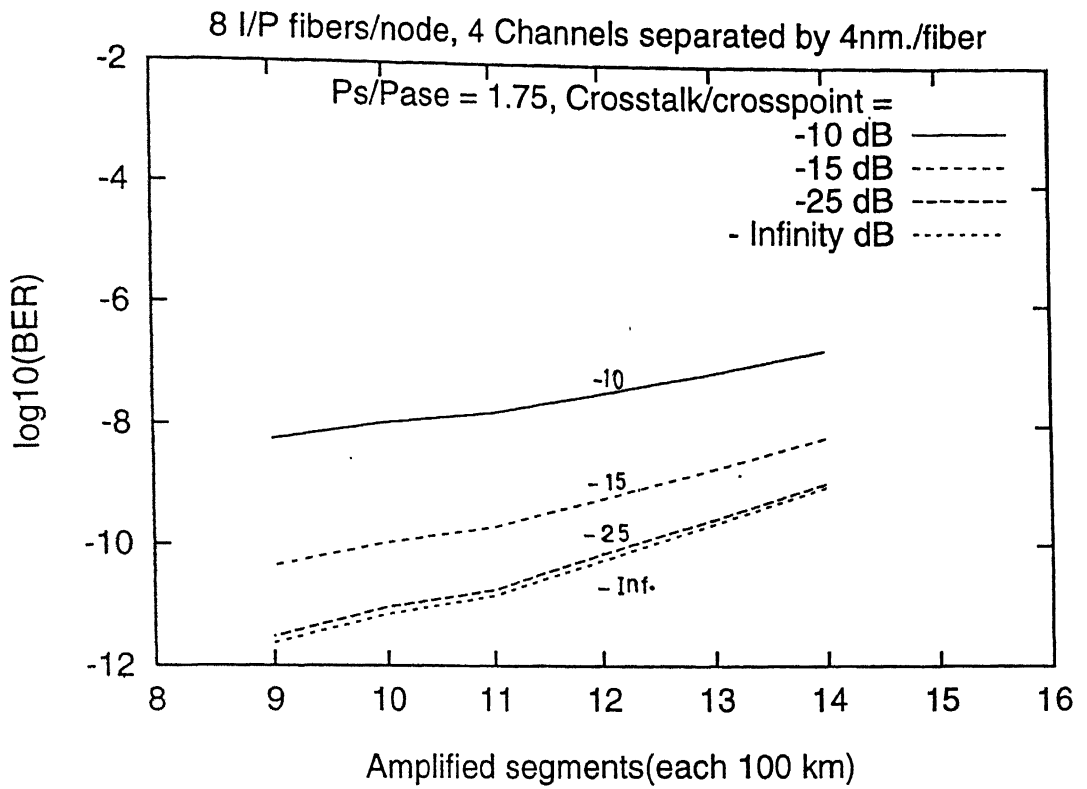
Fig. 6.3   BER Vs system length for different values of crosstalk/crosspoint . (N = 4, $\Delta f = 4$nm., La = 100 k

8 I/P fibers/node, 8 Channels separated by 1nm./fiber

Ps/Pase = 1.75, Crosstalk/crosspoint =
-10 dB ———
-15 dB - - - - -
-25 dB — — —
- Infinity dB ·········
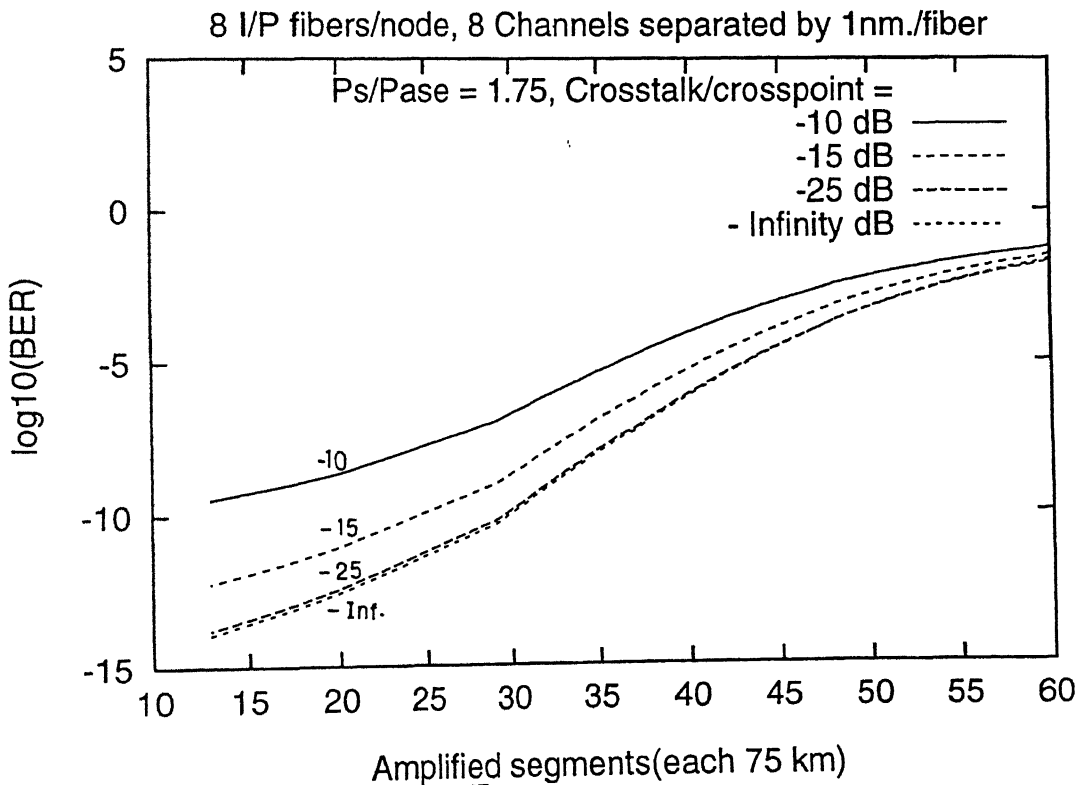
Fig. 6.4   BER Vs system length for different values of crosstalk/crosspoint . (N = 8, $\Delta f = 1$nm., La = 75 km

8 Channels separated by 1nm./fiber,X-talk/x-point = -10dB
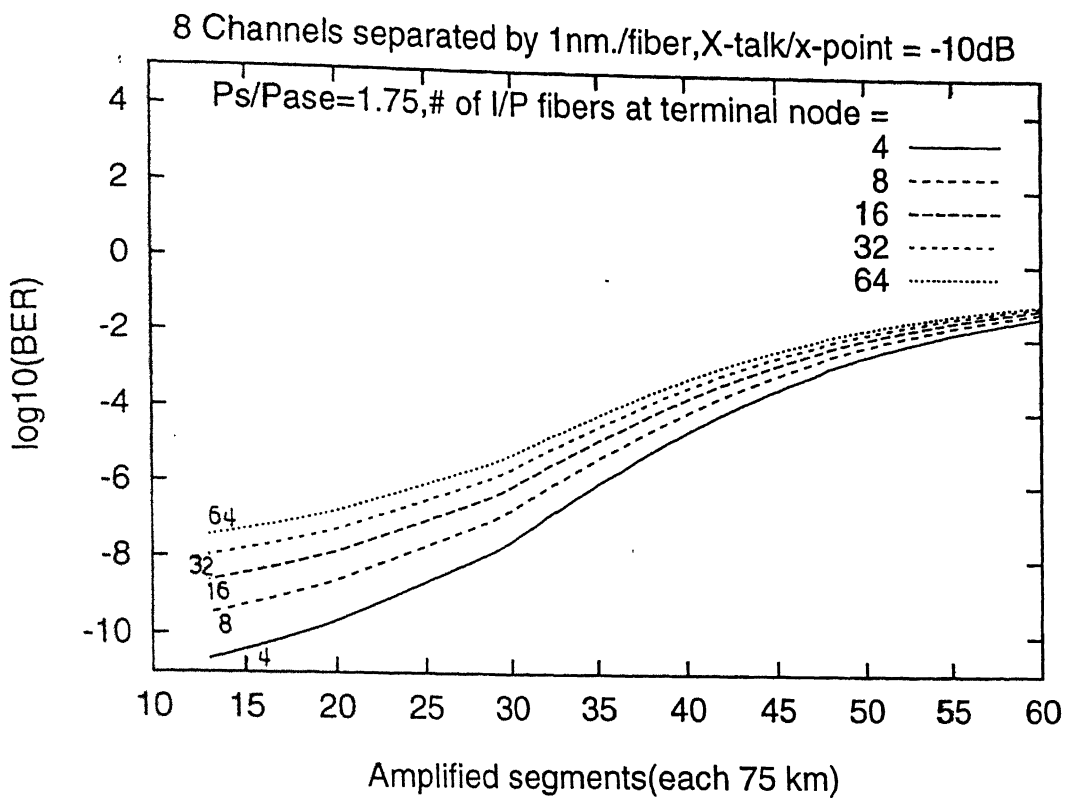
Fig. 6.5   BER Vs system length for different number of input fibers at a node (N = 8, $\Delta f = 1$nm., La = 75 k

4 Channels separated by 4nm./fiber,X-talk/x-point = -10dB

Fig. 6.6   BER Vs system length for different number of input fibers at a node (N = 4, $\Delta f = 4$nm., La = 100 km)

CHAPTER - 7

CONCLUSION

In this study, an attempt has been made to study the effects of the SRS, FWM, amplifier spacing. ASE noise, channel separation, number of channels, coupled power and the optical space switch crosstalk on the performance of WDM fiber optic systems. BER has been calculated and the effects of all the above mentioned factors on it studied for a WDM system shown in Fig. 1.4.
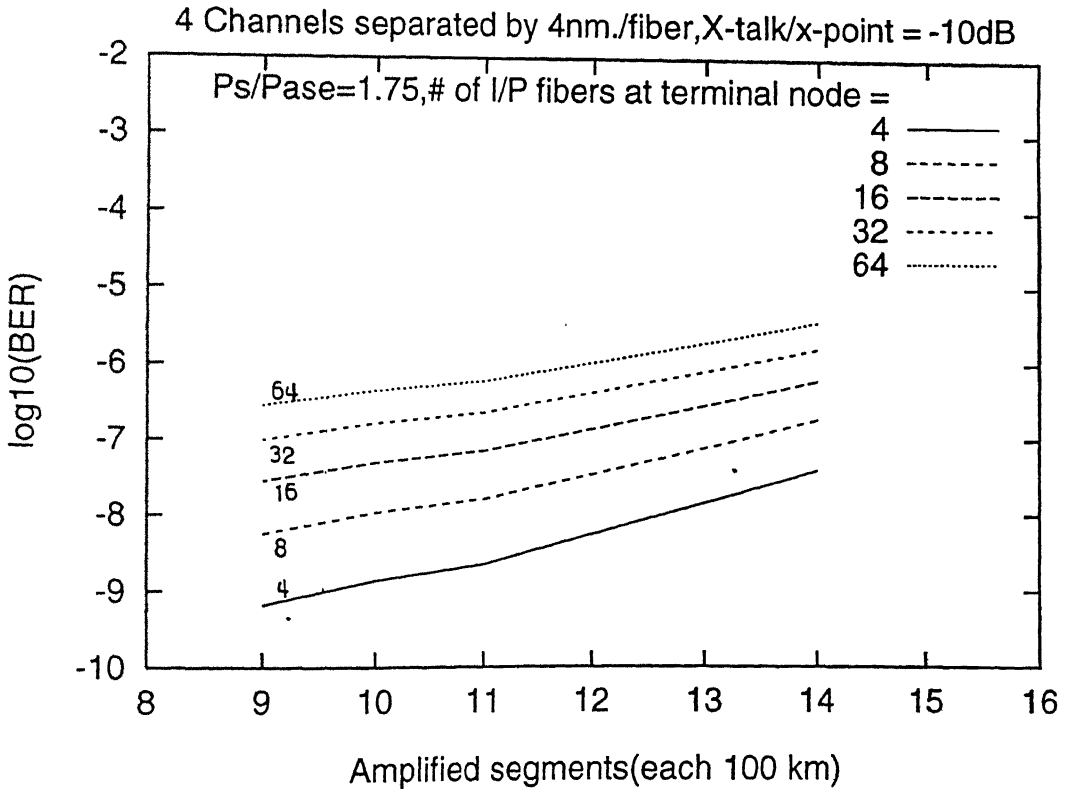
7.1 OBSERVATIONS

In Chapter 2, it has been observed that with a decrease in amplifier spacings both the FWM and the SRS effects increase. With an increase in the number of channels the maximum power allowed per channel to keep the SRS effect at the minimum decreases, but, the maximum power allowed per channel to keep the FWM effect at the minimum remains almost constant. Whereas a decreases in the channel separation has the opposite effect on SRS and FWM, i.e., with a decrease in the channel separation the maximum power allowed per channel to keep the SRS effect at the minimum increases, but, the maximum power allowed per channel to keep the FWM effect at the minimum decreases. So a suitable compromise in the selection of the number of channels, the channel separation and the amplifier spacing may have to be made for designing efficient WDM systems.

In Chapter 3, it is seen that with a decrease in the amplifier spacing, for a given system length, total accumulated ASE noise power decreases, but, at the same time the end-to-end

system bandwidth also decreases, which is not desirable. So the choice of the amplifier spacing is not straight forward as it depends on the required end-to-end bandwidth which in turn depends upon the number of channels and channel separation. The number of channels and channel separation further vary the FWM and SRS effects. So all this interdependence makes the designing of an efficient WDM system complicated.

In chapter 4, it has been shown that the coupled power plays a crucial role in keeping the effects of SRS and FWM at the minimum and deciding the maximum achievable system length. Two cases, each with 4 channels, but with different channel spacings of 4 nm and 1 nm, have been considered. As shown in Figs. 4.6 and 4.7, in the 4 nm channel spacing case the SRS effect is dominant and limits the system length to just 700 km, but, with a decrease in the coupled power $P_{S,O}$ (equal to output power for each amplifier) from about 32 mW to about 22.5 mW, the system length increases to 1000 km. But, further decrease in the $P_{S,O}$ does not give any additional increase in the system length. In the case of 1 nm channel separation, FWM is dominant and limits the system length to just 200 km. System length increases to 800 km with a decrease in $P_{S,O}$ to about 5 mW.

In chapter 5, for the WDM system shown earlier in Fig. 1.1, the BER has been calculated taking into account the combined effect of the number of channels, channel separation, amplifier spacing, coupled power, SRS, FWM and ASE noise. It has been observed that the limits on the system length imposed by the FWM and SRS effects, as discussed in chapter 4, can be exceeded. The extent to which these limits can be exceeded depends upon the BER

requirement. It is seen from Figs. 5.3 to 5.5, that for a WDM signal consisting of 4 channels with 4 nm channel separation, each having a data rate of 2.5 Gbits per second and for P_S/P_{ase} = 1.75, the maximum achievable system length for BER = 10^{-10} is 1200 km, 1950 km and 2600 km for the amplifier spacing of 100 km, 75 km and 50 km, respectively. So the 50 km amplifier separation is the best in this case as it gives the maximum system length.

In Figs. 5.7 and 5.8, for the WDM signal consisting of 12 channels separated by 1 nm, for BER = 10^{-10}, the system length achieved is about 1700 km for both the 50 km and 75 km amplifier separations. So the choice of amplifier separation is dependent on both the number of channels and the channel separation. Also in Fig. 5.11 for a WDM signal consisting of 16 channels separated by 1 nm, a saturation in BER in the 11th segment (each segment 75 km long) for $P_S/P_{ase} \simeq 5$ is observed. This indicates that an increase in the coupled power does not always improve the system performance. The reason is that when the power limits imposed by the SRS and the FWM are exceeded by increasing the coupled power, the SRS and FWM effects increase and at a certain point the increase in the SRS and FWM matches the increase in the signal power which leads to a saturation in the BER value.

In chapter 6, degradation of the system performance due to crosstalk in the space switches has been studied. It has been observed that the space switches with crosstalk level per cross point equal to -25 dB degrades the system performance almost negligibly. So for the large networks with a large number of space switches in an optical path, space switches with crosstalk per cross point less than -25 dB are required to avoid degradation

of the system performance.

For intensity modulation direct detection optical transmission, in the absence of dispersion compensation techniques, the maximum distance dictated by linear dispersion is estimated by [15]

$$B^2 L \leq \frac{C}{2D\lambda^2}$$

where B is the bit rate and L is the system length.

In this study, intensity modulation direct detection optical transmission in dispersion shifted optical fiber is considered for dispersion coefficient D = 2 ps/nm-km and data rate of 2.5 Gbits/sec, the distance of approximately 5×10^3 km would be theoretically possible. Since the maximum distance considered in the calculations is 3×10^3 km, well below the limit 5×10^3 km, the effect of chromatic dispersion on the system performance is not taken into account.

During the calculations of BER it has been noticed that for a WDM signal consisting of four channels and 4 nm channel separation for P_S/P_{ase} = 2 and coupled power of 33 mW, BER at the output of the receiver taking shot noise and thermal noise variance also into account is $10^{-11.274733}$ at the 13th segment (amplifier spacing = 100 km), and neglecting the shot noise and thermal noise the BER is $10^{-11.274389}$. So the BER value changes negligibly by including shot noise and thermal noise along with other effects. The reason for this is that the average shot noise and thermal noise powers are much less in comparison to other beat noise powers, even though the noise powers given above are the worst case values. So in the calculations of BER thermal and shot noises are neglected.

7.2 SUGGESTIONS FOR FURTHER WORK

Instead of keeping the channel separation constant in a WDM system, if it is varied, it will decrease the FWM effect as the probability of matching of the newly generated frequencies due to this effect with already existing ones will decrease. Also the SRS effect will vary in such a case. The effect on system performance due to such nonuniform channel separation can be studied.

With a change in amplifier spacing the gain requirement of the inline amplifiers changes which in turn varies the ASE noise accumulation. Also it changes the FWM and SRS effects due to a change in the overall effective length of the system. So it will be interesting to study the effect of nonuniform segment lengths on the system performance.

REFERENCES

1. G. P. Agarwal, "Nonlinear Fiber Optics", Academic Press, New York, 1989.

2. A. R. Chraplyvy, "Limitations on Lightwave Communications Imposed by Optical - Fiber Nonlinearities", *Journal of Lightwave Technology*, Vol. 8, No. 10, Oct. 1990, pp. 1548-1557.

3. A. R. Chraplyvy, "Optical Power Limits in Multi-channel Wavelength - Division - Multiplexed systems due to Stimulated Raman Scattering", *Electronic Letters*, Vol. 20, No. 2, Jan. 1984, pp. 58-59.

4. Mari W. Maeda, W. B. Sessa, W.I. Way, A. Yi-Yan, L. Curtis, R. Spicer and R. I. Laming, "The Effect of Four - Wave Mixing in Fibers on Optical Frequency - Division Multiplexed Systems", *Journal of Lightwave Technology*, Vol. 8, No. 10, Sep. 1990, pp. 1402 - 1408.

5. M. J. O'Mahony, A. Yu, J. Zhou, "The Design of a European Optical Networks", *Journal of Lightwave Technology*, Vol. 13, No. 5, May 1995, pp. 817-828.

6. S. Shimanda and H. Ishia, "Optical Amplifiers and their Applications", John Wiley and Sons, New York, 1992.

7. C. R. Giles, E. Desurvire, "Propagation of Signal and Noise in Concatenated Erbium-Doped Fiber Optical Amplifiers", *Journal of Lightwave Technology*, Vol. 9, No. 2, Feb. 1991, pp. 147-153.

8. C. R. Giles, E. Desurvire and J. R. Simpson, "Transient Gain and Crosstalk in Erbium Doped Fiber Amplifiers", *Opt. Lett.*, Vol. 14, No. 16, 1989, pp. 880-882.

9. G. R. Hill, "A Transport Network Layer Based on Optical Network Elements", *Journal of Lightwave Technology*, Vol. 11, No. 5/6. May/June 1993, pp. 667-676.

10. N. A. Olsson, "Lightwave Systems With Optical Amplifiers", *Journal of Lightwave Technology*, Vol. 7, No. 7, July 1989, pp. 1071-1082.

11. Kyo Inove, "A Simple Expression for Optical FDM Network Scale Considering Fiber Four-wave Mixing and Optical Amplifier Noise", *Journal of Lightwave Technology*, Vol. 13, No. 5, May 1995, pp. 856 - 860.

12. R. Gangopadhyay, S. P. Mazumder, G. Prati, "Impact of Four Wave Mixing in Dense WDM Switched Optical Network", *Proceedings of National Symposium on Fiber Optic Communication Networks and Sensors*, I.I.T. Kanpur, 1995.

13. C. Saxtoft and P. Chidgey, "Error Rate Degradation Due to Switch Crosstalk in Large Modular Switched Optical Networks", *IEEE Photonics Technology Letters*, Vol. 5, No. 7, July 1993, pp. 828-831.

14. R. A. Spanke, " Architectures for Guided Wave Optical Space Switching Systems", *IEEE Communication Magazines*, Vol. 2.5, No. 5, May 1987, pp. 42-48.

15. P. Henry, "Lightwave Primer", *IEEE J. Quantum Electronics*, Vol. QE-21, No. 12, 1985, pp. 1862-1879.